Cretaceous Volcanic Sequences And Jurassic Oceanic Crust In The East Mariana And Pigafetta Basins Of The Western Pacific

L. J. ABRAMS AND R. L. LARSON

Graduate School of Oceanography, University of Rhode Island
Narragansett, RI

T. H. SHIPLEY

Institute for Geophysics, University of Texas
Austin, TX

Y. LANCELOT

Laboaratoire de Geologie du Quaternaire, CNRS-Luminy
Marseille, France

We report the results of the first regional multichannel seismic studies of both the East Mariana and Pigafetta basins of the western Pacific which imaged oceanic crust, mapped the overlying strata and identified a site where Ocean Drilling Program (ODP) Leg 129 recovered Jurassic sediments and oceanic crust for the first time in the Pacific. The calibration of our seismic surveys and the extrapolation of drilling results throughout these oldest Pacific basins indicate that the flat-lying, high-amplitude reflection known as Horizon B corresponds to the top of middle Cretaceous flows/sills that overlie Jurassic/ Early Cretaceous sediments and oceanic crust throughout an area ~ 500,000 km^2 in the East Mariana Basin and the southeast Pigafetta Basin. Seismic refraction and reflection data allow an estimate of 400 m for the maximum thickness of these flows/sills. A distinct change in the reflection character of Horizon B from flat-lying and "smooth" to higher relief and "rough" observed in the southeast Pigafetta Basin marks the change from middle Cretaceous sills/flows overlying Jurassic oceanic crust to oceanic crust without a massive igneous overburden. Jurassic oceanic crust and overlying Upper Jurassic - Lower Cretaceous sediments unquestionably exist at ODP Site 801 in the Pigafetta Basin and are intermittently covered by sills/flows over the 550 km between Site 801 and Site 800. The Ogasawara Fracture Zone, which separates the East Mariana Basin and Pigafetta Basin, acted as a locus for middle Cretaceous volcanic activity as indicated by the coincident alignment and age of seamounts. Intrabasin morphotectonic features other than seamounts which could represent a possible source for the extensive cover of deep sea sills and flows are not obvious on seismic or bathymetric records. The ubiquitous presence of middle-to-Late Cretaceous volcanogenic turbidites and widespread occurrences of middle Cretaceous deep sea sills/flows throughout these basins indicate a pulse in voluminous off-ridge volcanic activity beginning in late Barremian/early Aptian.

INTRODUCTION

Magnetic anomaly sequences indicate that the world's oldest in situ ocean crust lies centered in the far western Pacific [Larson and Chase, 1972; Hilde et al., 1976; Larson, 1976]. An area, approximately the size of the contiguous United States, enclosed by the M17 isochron is inferred to contain oceanic crust and sediment of Jurassic age (Figure 1). Prior to ODP Leg 129 (Nov-Jan 1989-90), no Jurassic material had been sampled within this region by eight scientific drilling legs since 1969 and numerous dredging expeditions beginning in the 1950's. Instead the oldest material recovered has almost invariably been of mid- to Late Cretaceous age and often volcanic in origin. The results from the earliest drilling expeditions led Winterer [1976] to conclude that the recovered basalts probably buried older Early Cretaceous-Jurassic sediments and oceanic crust in the deep portions of western Pacific basins. This hypothesis represented one aspect of Menard's [1964] "Darwin Rise" which calls for the emplacement of abyssal flood basalts in Cretaceous time in order to account for the burial of abyssal hills surrounding Cretaceous seamounts.

The Mesozoic Pacific: Geology, Tectonics, and Volcanism
Geophysical Monograph 77

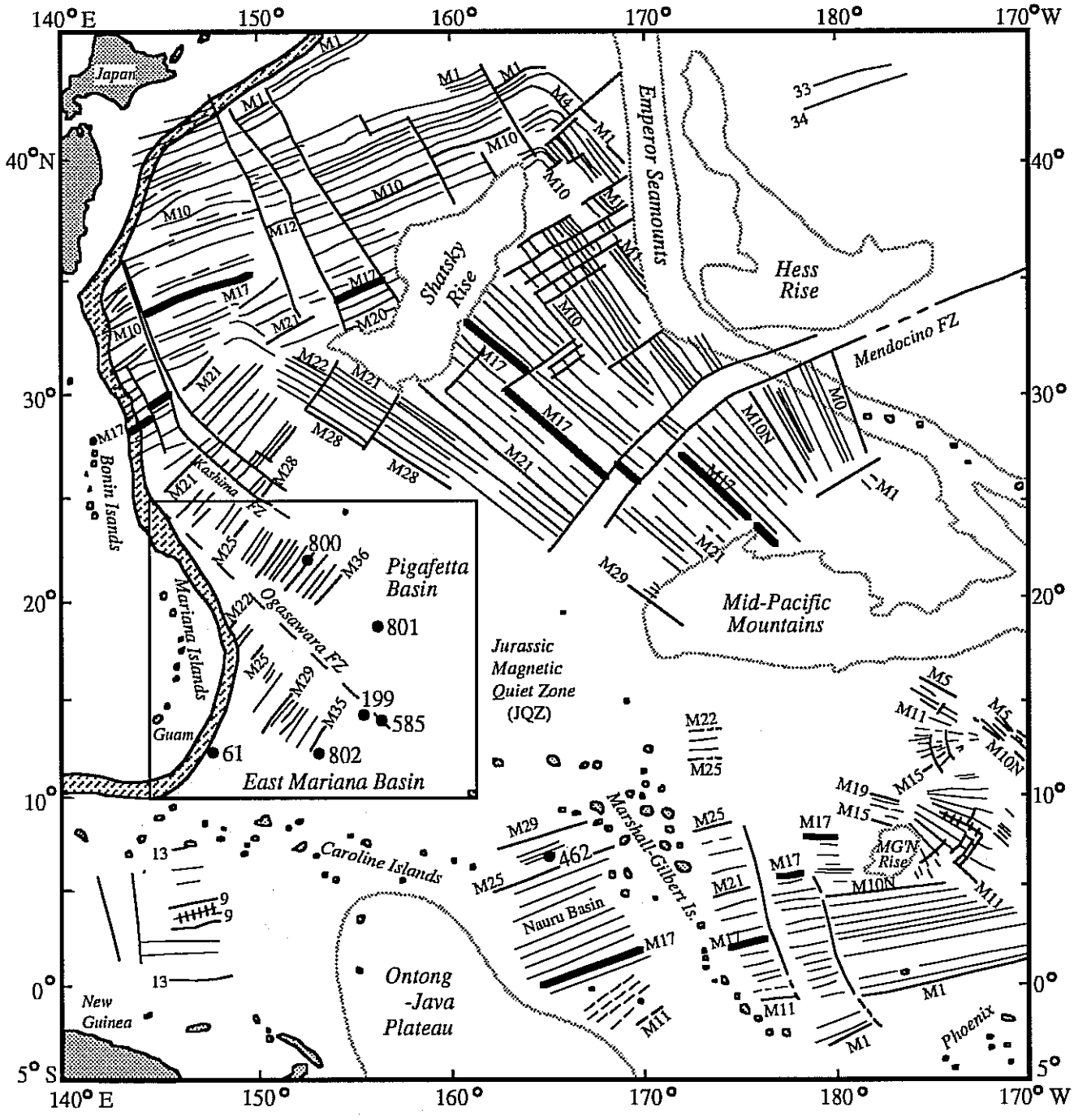

Fig. 1. Magnetic lineations of the western Pacific compiled by R. L. Larson from Hilde et al. [1976], Larson [1976], Weissel and Anderson [1978], Mammerickx and Sharman [1988], Tamaki and Larson [1988], Handschumacher et al. [1988], and Sager et al. [1988], Nakanishi et al. [1989]. Magnetic isochron M17 is highlighted and approximates the Cretaceous - Jurassic boundary. Dots locate selected DSDP Sites 199, 585, 462 and all of ODP Leg 129 Sites 800, 801 and 802. Boxed region is shown in Figures 2, 4 and, 7.

The middle Cretaceous volcanism affecting these Jurassic basins manifested itself in several ways. Volcanism is associated with chains of seamounts and islands such as the Magellan and Marcus-Wake seamounts, which were near or above sea level by early Aptian (~124 Ma) [Moberly and Schlanger et al., 1986; Lancelot and Larson et al., 1990; Winterer et al., this volume], the Mid-Pacific Mountains of Barremian to Campanian age (~132-74 Ma) [Hamilton, 1956;

Winterer and Ewing et al., 1973; Thiede and Vallier et al., 1981], and the Marshall/Gilbert Seamounts of at least Albian to Paleocene age (112-56.5 Ma) [Lincoln et al., this volume; Haggerty and Primoli Silva, et al., in press]. There is also excess mid-plate volcanism in the form of huge oceanic plateaus such as the Ontong-Java Plateau of earliest Aptian age (~124 Ma) [Kroenke and Berger et al., 1991; Tarduno et al., 1991]. Finally, the most poorly mapped and dated mid-plate volcanism in the form of deep-sea sills and flows (Nauru Basin - Larson and Schlanger et al., 1981; Central Pacific Basin - Winterer and Ewing et al., 1973; East Mariana and Pigafetta basins - Lancelot and Larson et al., 1990). The extent of this mid - to Late Cretaceous deep sea volcanism, its relationship to numerous seamounts, guyots, underlying sediments, and oceanic crust are of primary concern in this study.

Seismic reflection and refraction studies of the East Mariana Basin (EMB) and Pigafetta Basin (PB) presented in this paper show images of oceanic crust, define its seismic structure, map the overlying strata and identify a site where the D/VJOIDES Resolution was able to recover Jurassic oceanic crust during ODP Leg 129 [Abrams et al., 1988; Lancelot and Larson et al., 1990]. The successful completion of Leg 129, resulting in the first and only holes to penetrate igneous basement (middle Cretaceous basalt or Jurassic oceanic crust) in the EMB and PB, allowed the calibration of this extensive MCS and SCS data set, the extrapolation of drilling results throughout these basins and comparisons with other western Pacific basins of Jurassic age (e.g. Nauru Basin see Shipley et al., this volume). This basinwide correlation permits a physical and age determination of the flat-lying, high-amplitude reflection(s) known as "Horizon B" or "reverberant layer", observed in extensive areas of the western Pacific including the EMB and PB. These results enable us to place geologic age and volumetric bounds on deep sea volcanism in the EMB and PB and to discuss its relationship with the worldwide occurrence of voluminous middle Cretaceous volcanism.

TECTONIC SETTING

The bathymetric map of this region (Figure 2) reveals a huge area (~ 1 x 10^6 km^2) at depths greater than 5500 m, which we consider the EMB and PB. The EMB is bounded to the west-northwest by the Mariana Trench, to the southwest by the Caroline Ridge, and to the northeast by the northwest-trending Ogasawara Fracture Zone and Magellan Seamounts [Tamaki et al., 1987; Handschumacher et al., 1988] (Figures 1 and 2). The PB is bounded to the northeast by the Kashima Fracture Zone and Marcus-Wake Seamounts and to the southeast by the Ogasawara Fracture Zone and Magellan Seamounts and extends to the northwest, where it terminates at the Bonin Trench.

In this paper age is assigned according to the Harland et al. [1990] geologic time scale. The younger parts of the EMB toward the northwest are believed to be Kimmeridgian to Oxfordian (anomalies M22 to M25, ~150 - 155 Ma) and just seaward of the Bonin Trench the PB may be as young as Valanginian-Tithonian (M13-M17, ~139-145 Ma). Within our survey area the central parts of these basins are extrapolated to be Oxfordian to Callovian (anomalies M29 to M36, ~157-161 Ma) and toward the southeast, within the so-called Jurassic magnetic quiet zone (JQZ), the age of the crust may be as old as Bathonian to Bajocian (Middle Jurassic, ~161-174 Ma) [Tamaki et al.,1987; Handschumacher et al., 1988; Nakanishi et al., 1989; and Nakanishi et al., 1992]. These inferences were confirmed by the 166.8 +/- 4.5 m.y. age and geochemical attributes of the tholeiitic basalts recovered at Site 801 in the JQZ that indicate they represent Jurassic oceanic crust [Floyd et al., 1991; Pringle, 1992a; Castillo et al., 1992]. The exact nature of the low field uncorrelated magnetic anomalies in the JQZ remains unknown, but the equivalent time interval in land sections was found to be a period of extremely frequent magnetic reversals by Steiner et al. [1987]. A crustal age of ~167 Ma at Site 801 results in pre-M25 half-spreading rates of approximately 80 mm/yr assuming constant rates of spreading and an M25 date of 155 Ma [Harland et al., 1990]. This spreading rate is comparable to the fastest half-spreading rates presently documented on the East Pacific Rise (80 - 90 mm/yr, Macdonald, 1982).

PREVIOUS STUDIES

Western Pacific Seismic Stratigraphy

The seismic stratigraphy of large portions of the western Pacific including the PB and EMB consists of four units originally defined by Ewing et al. [1968]: (1) an upper transparent layer, (2) an upper opaque layer, (3) a lower transparent layer, and (4) Horizon B. This paper will concentrate primarily on the Horizon B reflection and sub-Horizon B velocity structure throughout the EMB and PB. The stratigraphy overlying Horizon B is discussed in Abrams et al. [1992].

Horizon B has been referred to as the "deep opaque layer" [Heezen and MacGregor et al., 1973], as the "reverberant layer" by Houtz et al. [1970] and Houtz and Ludwig [1979], and as "acoustic basement". Horizon B has been characterized from observations of SCS analog airgun profiles by the presence of a prominent zone of flat-lying ("smooth"), high-amplitude, and closely spaced reflections. Houtz and Ludwig [1979] completed an extensive review of the areal extent, thickness and velocity of the reverberant layer/Horizon B seismic facies throughout the western Pacific and speculated (as did Ewing et al., 1968) that this layer is composed of highly stratified calcareous or redeposited volcaniclastic sediments that overlie oceanic crust. Drilling in the western Pacific prior to Leg 129 has demonstrated that Horizon B can be produced by the impedance contrast between sediments and volcanic sills or flows (e.g. Nauru Basin-DSDP Site 462) and, in some cases, the sediment/oceanic crust interface in areas interpreted to contain particularly smooth crust. It is now recognized that the reverberant nature of Horizon B in airgun profiles is usually the result of a trailing bubble pulse oscillation reflecting from a high impedance boundary implying that the thickness or stratification inferred for this layer is an artifact of the airgun source and gain setting in the analog recording [Shipley et al., 1983]. This characteristic of

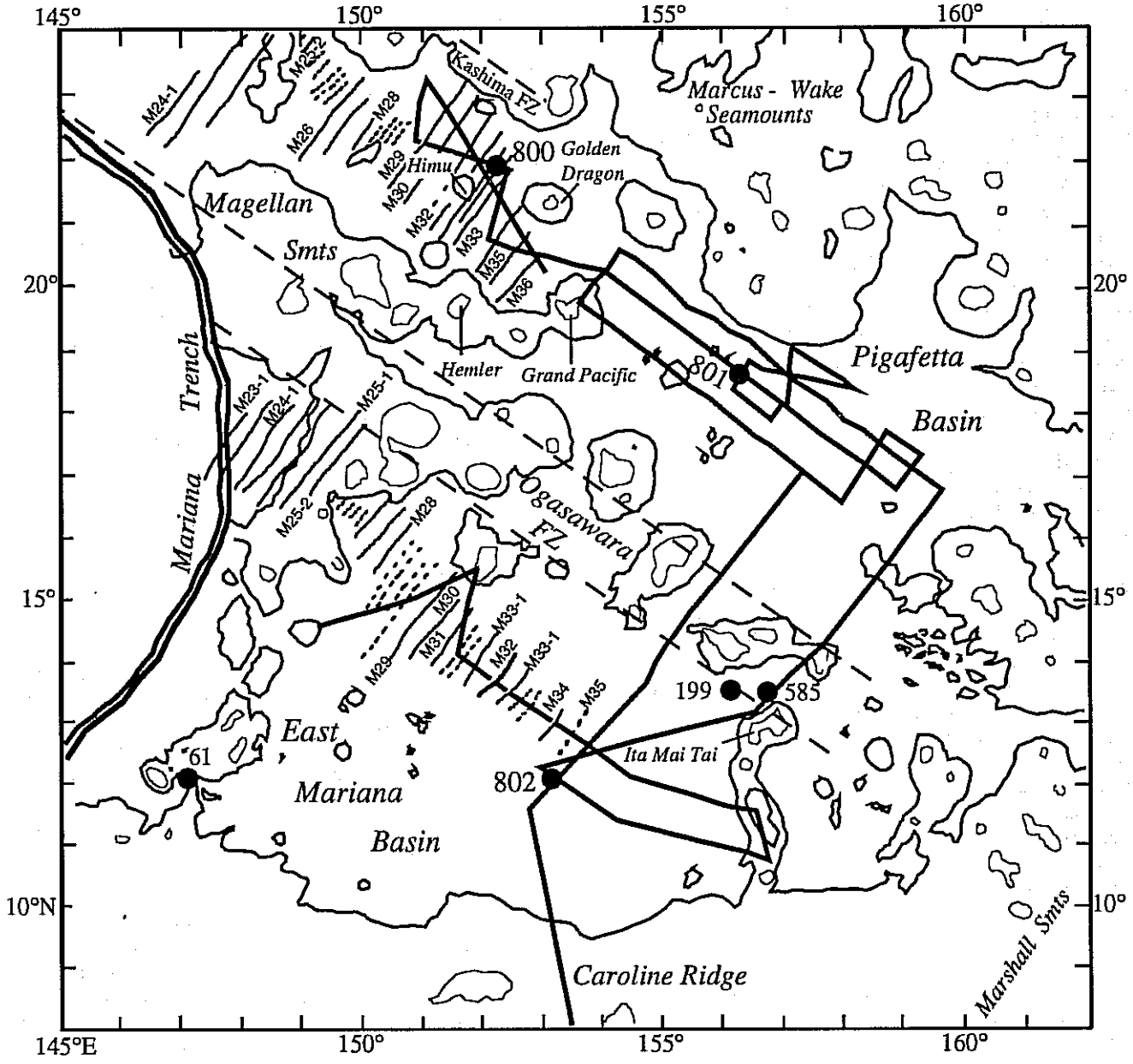

Fig. 2. Bathymetry of the central western Pacific modified from Brenner and Angell [1992] with location of selected DSDP sites and all of ODP Leg 129 sites. The 5500 m contour is highlighted and the 3000 m contour is shown as a lighter line. Magnetic anomalies modified from Tamaki et al. [1987] and Handschumacher et al. [1988]. The bold solid line indicates coverage of the MESOPAC II and FM35-12 seismic surveys. The broad area inferred for the location of the Ogasawara Fracture Zone is bounded by the dashed line.

the airgun source is now routinely compensated for through the use of tuned airgun arrays and/or deconvolution techniques and the use of waterguns, which provide a more implosive and bubble pulse-free source signature resulting in a high-resolution record with less processing effort [Hutchinson and Detrick, 1984].

Leg 129 Site Review

Sites drilled during ODP Leg 129 penetrated and recovered material correlated to all four general seismic units of Ewing et al. [1968], including Horizon B. The seismic stratigraphy at ODP Leg 129 Sites 800, 801, and 802 is summarized in Figure 3 (from Abrams et al. 1992).

Horizon B at all three Leg 129 Sites corresponds to the top of intrusive and/or extrusive dolerite/basalt at approximately 500 mbsf. In the northwest PB, at Site 800, dolerite sills radiometrically dated at 126.1 +/- 0.6 Ma intrude Berriasian (~140-145 Ma) pelagic sediment [Lancelot and Larson et al., 1990; Pringle, 1992]. Oceanic crust at Site 800, predicted to

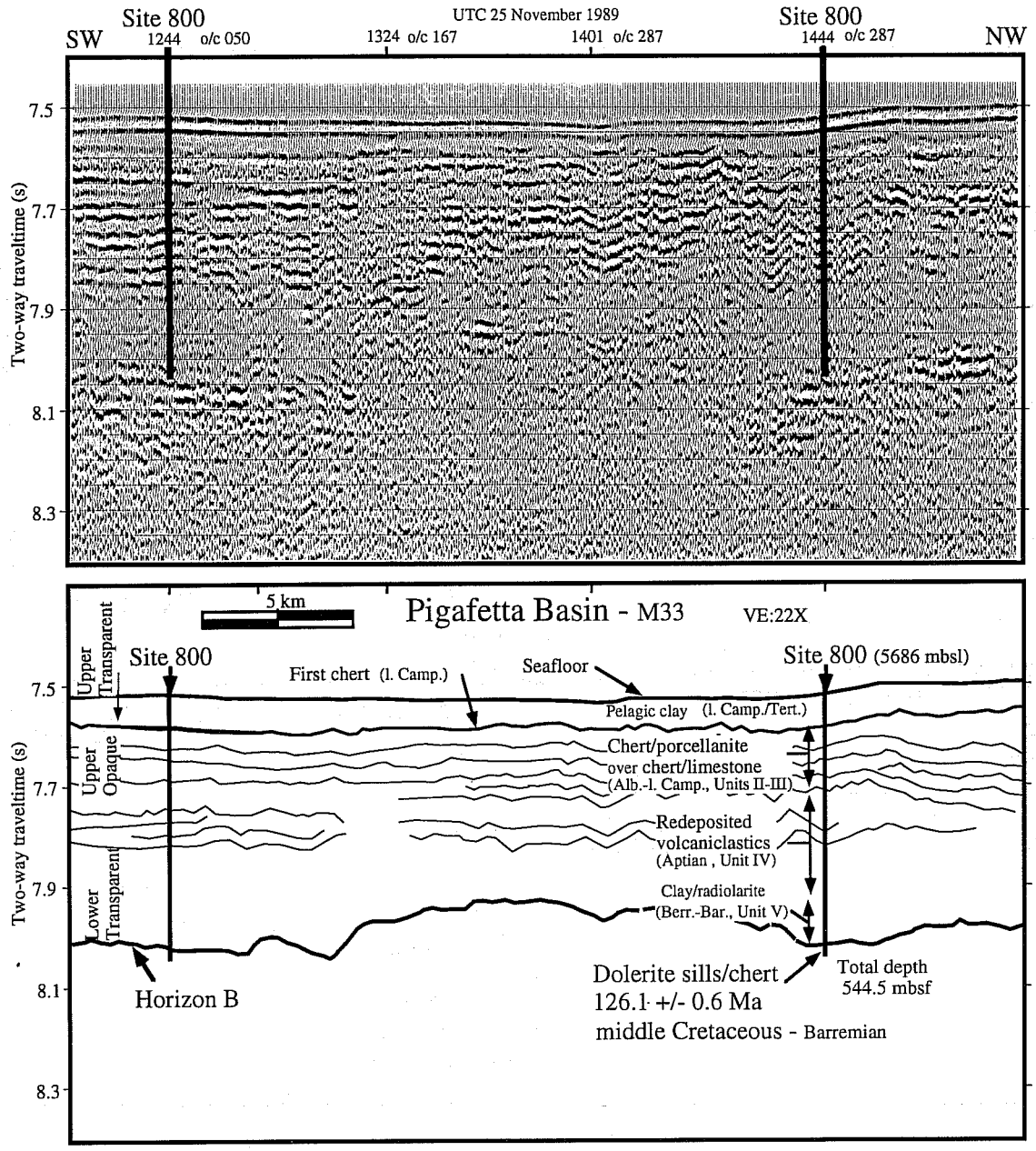

Fig. 3a.

Fig. 3a-c. Summary of seismic stratigraphy at ODP Leg 129 Sites 800 (a), 801 (b), 802 (c) showing generalized correlations with lithologic units, ages and depths, with emphasis on key reflective horizons such as igneous basement and shallowest chert ("first" chert) [Lancelot and Larson et al.,1990, Pringle, 1992]. Site 800 imaged with SCS waterguns (two 80 in^3) obtained on approach to Site 800 during Leg 129; seismic profiles for closest point of approach (CPA) to Sites 801 and 802 during MESOPAC II. These single channel watergun records were processed and displayed with the following parameters: water-velocity F/K migration, mute, 2-trace mix, band-pass filter 25-100 Hz, 500 msec AGC, and vertical exaggeration ~22X at 1.5 km/s. O/C = on course, UTC = Universal Time Code.

be ~ 160 Ma (M33), was not recovered. Horizon B at Site 802, in the central EMB, also correlates to a middle Cretaceous volcanic surface. At this location pillow and flow basalts dated at 114.6 +/- 3.2 Ma were recovered in an area where oceanic crust is predicted to be >161 Ma (M35). Site 801, in the JQZ of the PB is the only location where oceanic crust was recovered. The radiometric age (166.8 +/- 4.5 Ma, Middle Jurassic) of the tholeiitic basalt flows is almost exactly that predicted from linear extrapolation of post M25 magnetic lineations. Finally, thick sequences of middle to Late

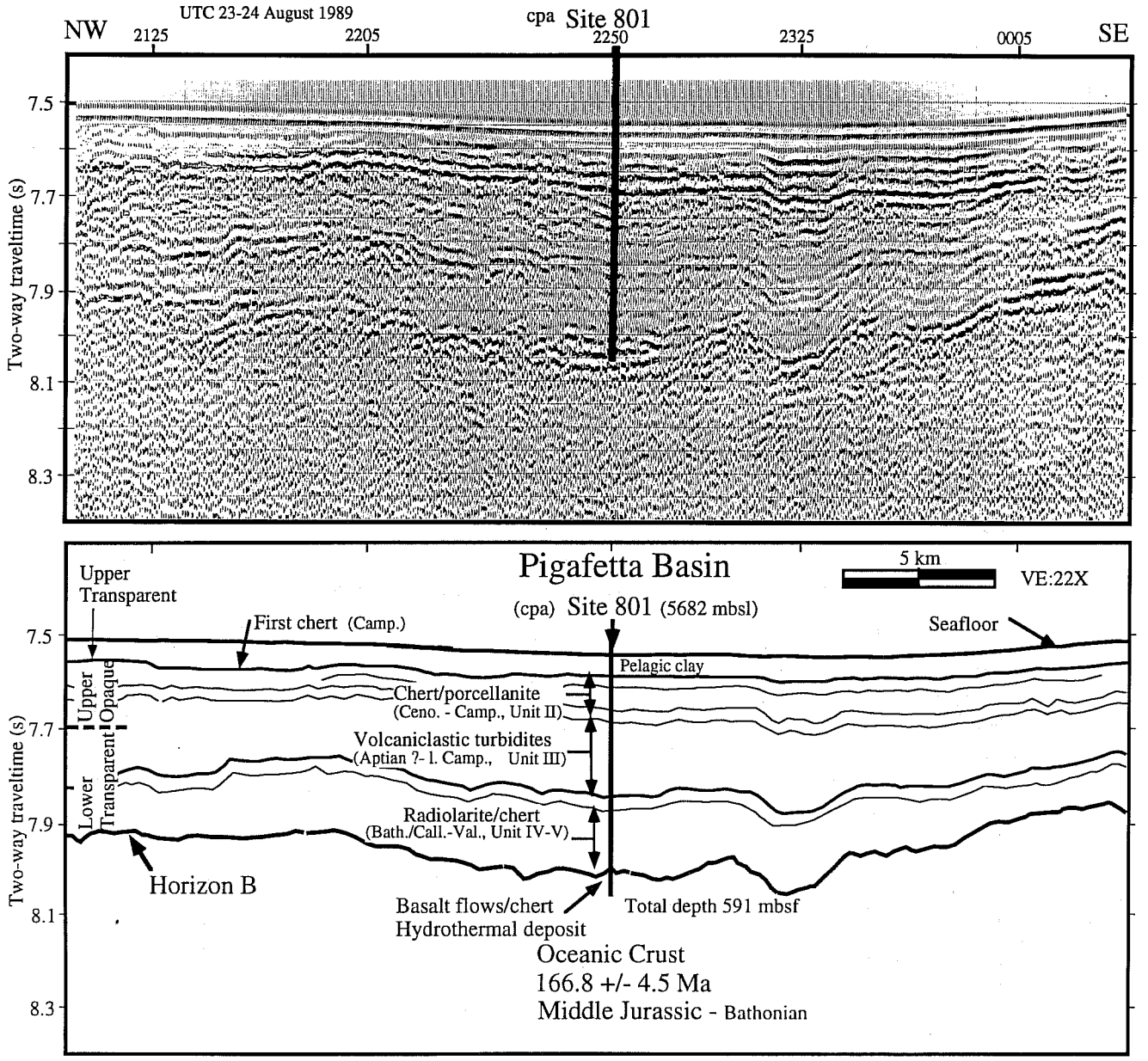

Fig. 3b.

Cretaceous volcanogenic turbidites were penetrated at all three Leg 129 sites as well as at DSDP Site 585, indicating that edifice building and emplacement of deep sea sills/flows (e.g., Sites 800, 802) were essentially synchronous [Lancelot and Larson et al., 1990]

DATA ACQUISITION AND PROCESSING

In November - December 1987 the R/V Fred H. Moore expedition FM35-12 collected over 3900 km of multichannel seismic (MCS) data using a 3200-m-long receiving array consisting of 96 hydrophone groups each 33.33 m in length (Figures 2 and 4). The seismic data were sampled at 4 ms, demultiplexed and recorded on a GUS 4200 Marine System. The Moore's seismic source consisted of various combinations of airguns fired at approximately 13.8 MPa (2000 psi) every 20 s. The maximum airgun volume achieved was 84.15 liters (5135 in^3) but the mean airgun volume during the 17 days of MCS acquisition was 40.65 liters (2481 in^3). Refraction data collected by seven long-range sonobuoys were also digitally recorded during this regional survey (sonobuoys 7, 8, 18, 20, 21, 22, 23). The MESOPAC II MCS survey conducted with the N/O Le Suroit during August - September 1989 focused on

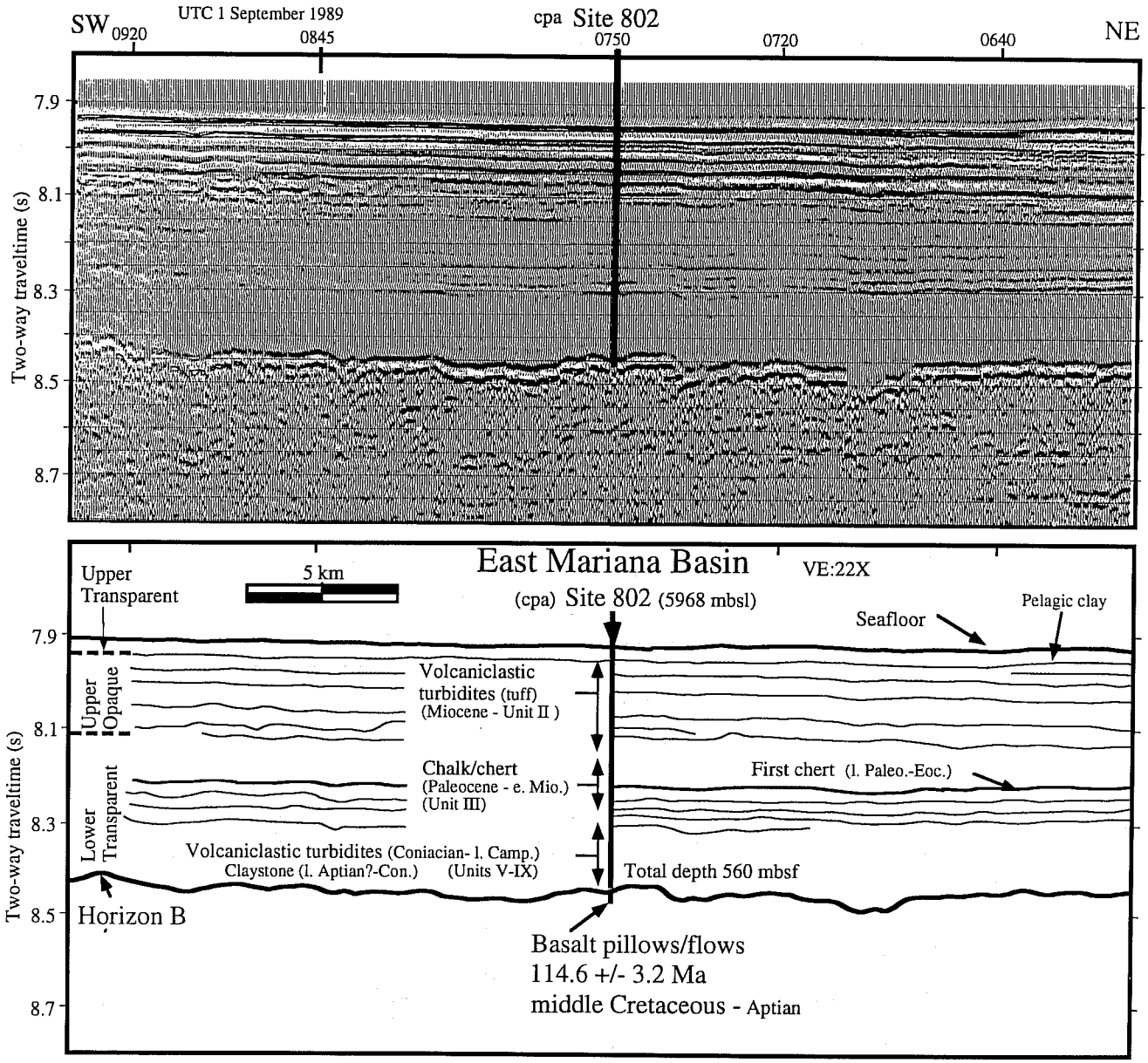

Fig. 3c.

potential drilling targets first identified on FM35-12 as well as investigating the northern PB within the oldest portion of the M-sequence lineation pattern. Only processed single channel data from MESOPAC II are used in this study. The MESOPAC II expedition also recorded approximately 3900 km of MCS data using an array of four to six 1.31 liter (80 in^3) waterguns fired every 13 s during vertical incident profiling and two 16.39 liter (1000 in^3) airguns fired every 31 s while digitally recording refraction data from six long-range sonobuoys (sonobuoys 1m, 2m, 3m, 4m, 6m, 8m).

During both cruises the ships maintained a speed of approximately 5 to 6 knots and navigated primarily by transit satellite but also by NAVSTAR global positioning system (GPS) with coverage of approximately 5 hours a day. Shot spacing was calculated for the FM35-12 data using final navigation along individual lines, and for MESOPAC II SCS watergun data was estimated at 40 m per shot. FM35-12 CDP gathers were created with 66.66-m bin size, 33.33-m hydrophone group spacing with variable shot spacing (~50 m/shot) resulting in 100 to 120 fold gathers. Stacking velocities from the seafloor to Horizon B were derived from semblance analysis of four adjacent CDP gathers at selected areas along each line and sub-Horizon stacking velocities were derived from sonobuoy results. Shot spacing for FM3512 and

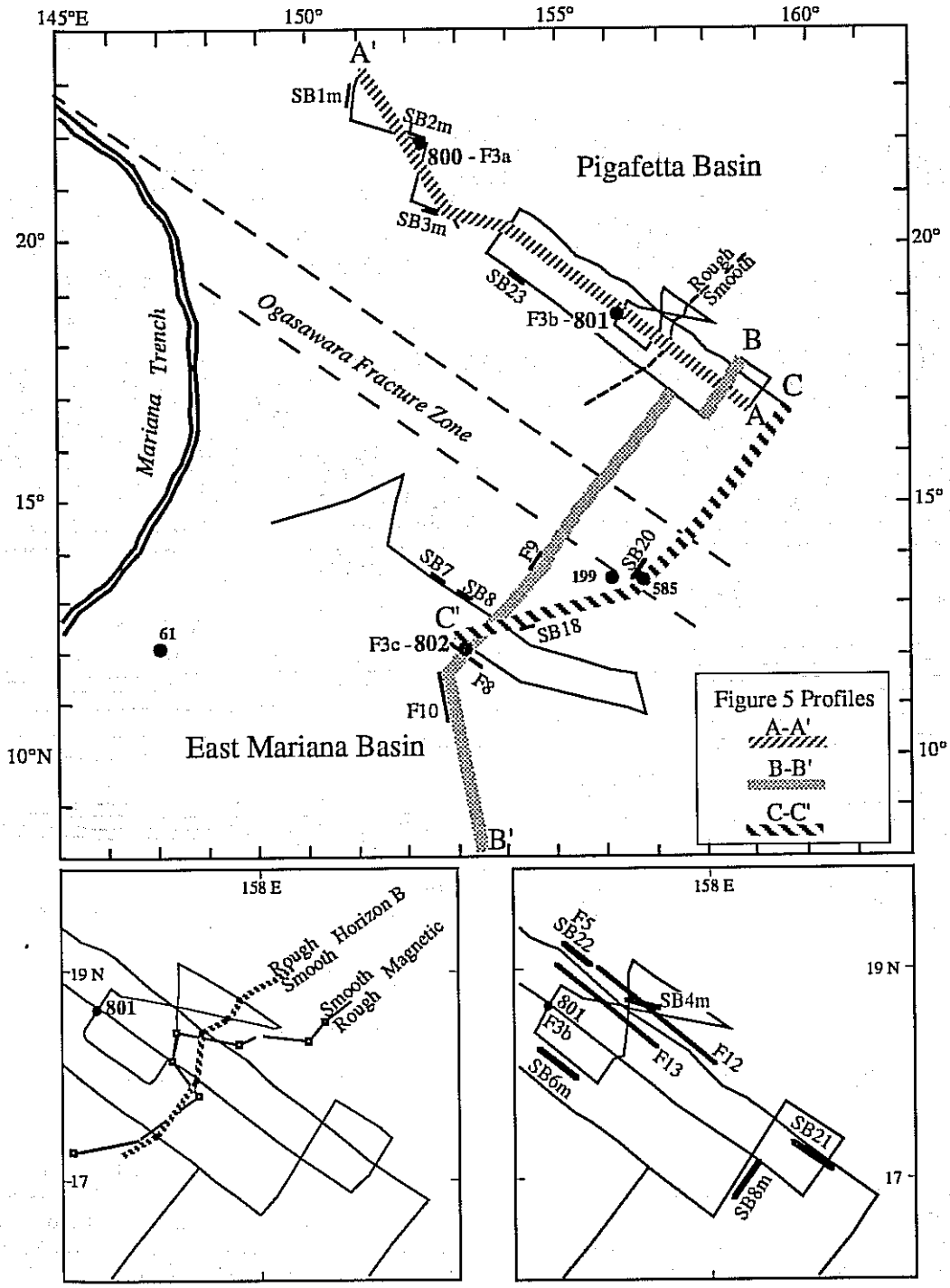

Fig. 4. Solid line indicates coverage of the FM35-12 and MESOPAC II regional seismic surveys with location of sonobuoy stations and transects in subsequent figures (heavy solid lines marked SB# and F# respectively). The endpoints of composite profiles shown in Figure 6 are marked A-A', B-B' and C-C' and highlighted as shown in the legend. The boxed region is enlarged and shown in two inset figures. The spatial relationship of rough/smooth Horizon B and the magnetic boundary as identified by Handschumacher et al. [1988] is shown in the left inset and the right inset more clearly displays track geometry and figure/sonobuoy locations. Dots show DSDP/ODP site locations.

MESOPAC II sonobuoys was 50-70 m and 80-90 m, respectively.

Sonobuoy Methods and Analyses

Travel time-range (T/X) data are used to determine the velocity beneath Horizon B, establish its relationship to the top of oceanic crust and define the general crustal structure throughout the EMB and PB. The sonobuoy T/X data from both FM35-12 and MESOPAC II were inverted to a layered velocity-versus-depth model by simply measuring the slopes and intercept times of first-arrival refractions and employing the Tau-p method of Diebold and Stoffa [1981]. This velocity model was used as a starting point for iterative forward modeling of T/X data using structures consisting of laterally homogeneous, constant velocity layers and/or constant velocity gradient. Observed T/X data were usually modeled within +/- 0.02 s, except for longer range mantle arrivals which have uncertainties on the order of 0.1 s. Amplitudes were not modeled, but relative amplitudes were used to qualitatively assess velocity gradients and to infer the location of critical points on mantle reflections in order to estimate mantle velocities and place further constraints on overlying velocities.

The primary limitations of this modeling technique are: (1) the assumption of one-dimensionality and, (2) the nonuniqueness of any "best fit" model, particularly the inherent ambiguity between variations in layer thickness and velocity in modeling travel time alone. The assumption of one-dimensionality with respect to topography appears justified in this area where the seafloor is essentially flat (+/- 75m maximum) over the 30-40 km range of these sonobuoys. The highest amplitude sub-bottom reflections are most often flat-lying but at some locations Horizon B displays up to 150 m of relief. There is also evidence on some sonobuoys for out-of-plane disturbances and discontinuities in basement structure. Direct wave arrivals were used to calculate ranges assuming a water velocity of 1.54 km/s estimated from CTD measurements. Sediment velocities, based on analysis of four contiguous CDP gathers from the 3.3 km-long 96-channel streamer, ranged from 1.6 to 3.0 km/sec, usually increasing with depth. This range in velocities is also consistent with modeled reflections within the sediment layer. Only one or two of the highest amplitude reflectors within the sediment were matched by velocity contrasts in the model, and sediments were divided into isovelocity layers even though it is recognized that velocity gradients may also occur.

In a few cases (e.g. sonobuoys 1m, 4m, 6m, 22) refracted second arrivals were observed within the reflection hyperbola of the seafloor and sediment and traced to their tangency to the Horizon B sub-bottom reflection (e.g., Figure 5). These continuously curved refractions are indicative of relatively steep velocity gradients and provide constraints on the velocity immediately below Horizon B. These refracted arrivals are continuous with high-amplitude first arrivals beyond 7 km range. In the remaining instances, where first arrival refractions could not be followed to shorter ranges within the seafloor reflection, a single velocity gradient was assumed, resulting in continuously curved modeled refraction arrivals tangent to the Horizon B reflection. The resulting velocities and velocity gradients are characteristic of oceanic layer 2. It was with this evidence that high-velocity igneous material was successfully predicted to occur at the depth of the Horizon B reflection at all three ODP Leg 129 Sites.

Oceanic layer 3 is well defined on many sonobuoys by the weak first arrivals beyond 18-20 km range (Figure 5). The relatively low amplitude of these refractions along with the high-amplitude reflection from the Moho indicate a low velocity gradient typical of oceanic layer 3 [White, 1979; Purdy, 1983]. The velocity at the bottom of layer 2 and top of layer 3 is constrained by arrivals between 10-20 km that are modeled as a layer with a small positive velocity gradient overlying a zero gradient layer 3. The velocity within layer 3 was usually assumed to be continuous with the overlying velocity structure.

Wide-angle mantle arrivals were modeled as reflection events from a single discontinuity in velocity at the layer 3/mantle interface. The distinct travel time separation between refracted arrivals from layer 3 (P3) and Moho reflections (PmP) places constraints on the thickness of layer 3, and therefore, total crustal thickness. The velocity and thickness of layer 3 were chosen to best fit the curvature and travel time of the Moho reflection. Reflections from the Moho also appear on FM35-12 CDP data at 1.8 to 2.2 stwt below Horizon B (10.1 - 10.5 stwt) and are used as further constraints on crustal thickness. The underlying mantle velocity is not well constrained by travel time data primarily because most sonobuoys were unable to record arrivals at ranges greater than 30 km, however upper mantle velocities of 8.2 km/s were recorded on ocean bottom seismometers (OBSs) from explosive charges at ranges from 50 to 500 km in the EMB [Asada et al., 1985]. In addition, the observed amplitude build up at 20-22 km range was used to estimate critical distance which required upper mantle velocities between 8.0-8.3 km/s for all of the models. Although the top of the Moho is well placed in these models, mantle arrivals over their entire range cannot be matched by a single discontinuity; the travel times in some cases are better fit by models which include a transition zone with a velocity gradient at the base of the crust.

SEISMIC OBSERVATIONS AND RESULTS

The results of our regional seismic profiles are illustrated in three cross sections (Figure 6) accompanied by several key seismic reflection examples. The cross sections were created by digitizing distinctive reflection surfaces which seemed to maintain unique characteristics (i.e. seismic facies) over basinwide distances. The selected horizons include the seafloor, the shallowest abundant chert/porcellanite/clay or chert/chalk, middle Cretaceous basaltic sills/flows and/or the top of Jurassic oceanic crust. The lithofacies significance of these distinct horizons and the intervals which they bound are based on the lithologies recovered during ODP Leg 129 as well as DSDP Sites 61, 199 and 585 [Abrams et al., 1992].

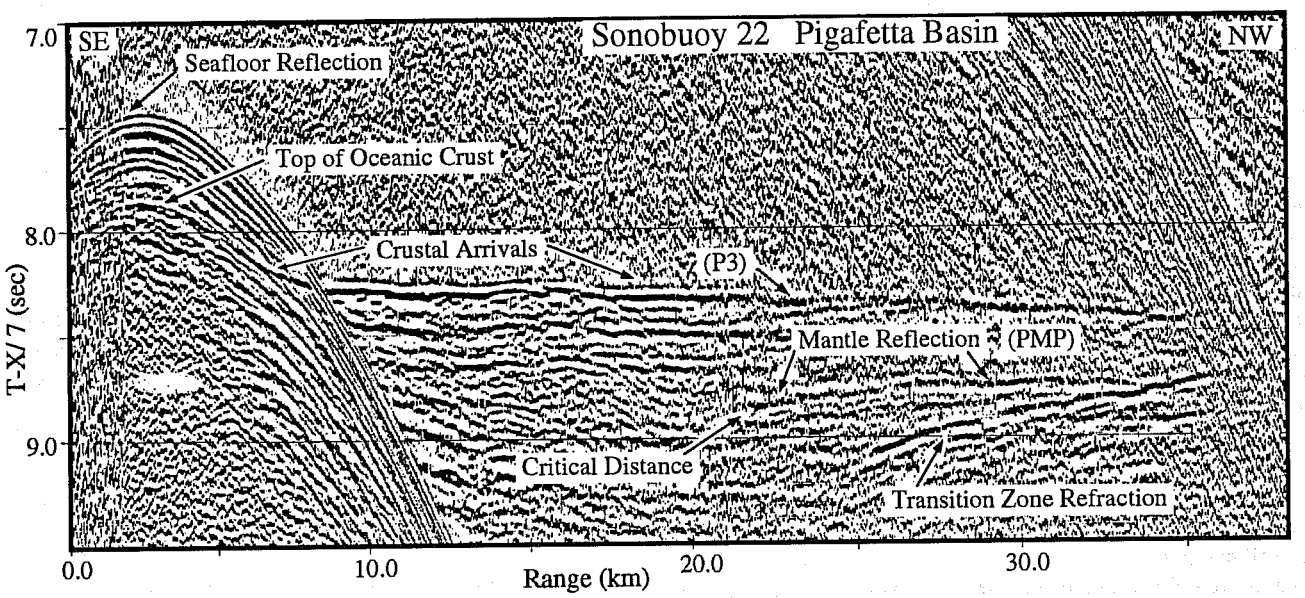

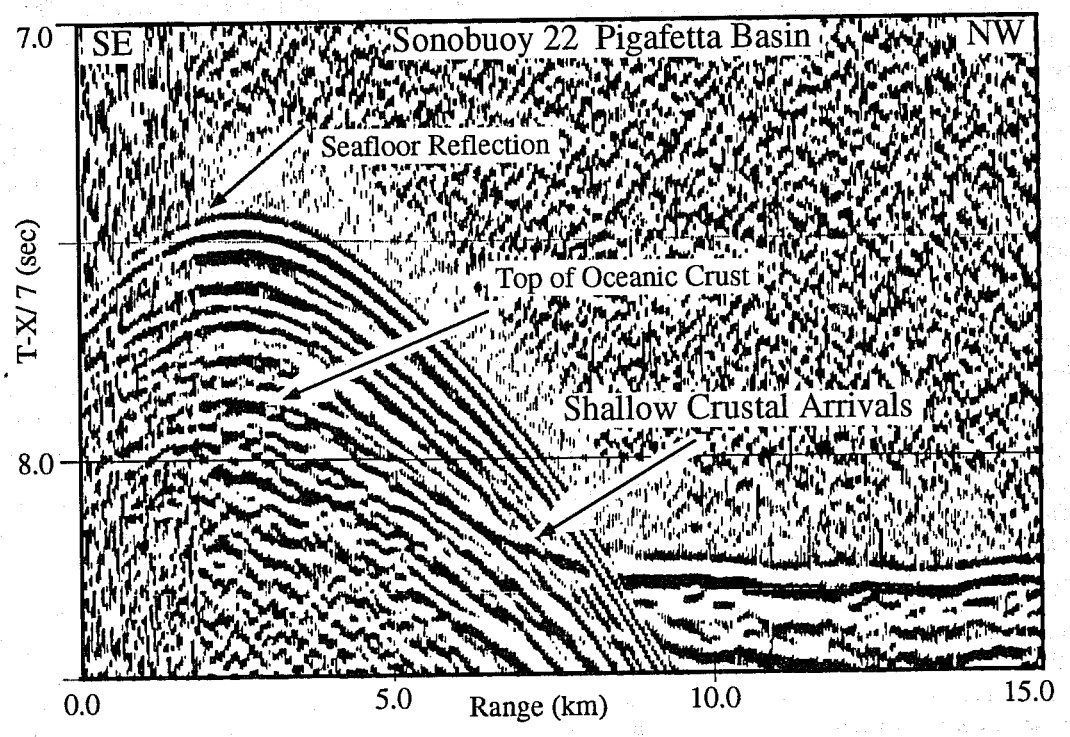

Fig. 5a-b. Traveltime - range data from sonobuoy 22 in the JQZ of the PB located 55 km Northwest of ODP Site 801 is shown at reduced travel time (7km/s), 500 msec AGC, band-pass filter 8-25 Hz. Figure 5a (top) displays entire record section out to 40 km range. Figure 5b (bottom) is an enlargement of this data from 0-15 km. Refracted/reflected arrivals of note are labeled. Refracted second arrivals (labeled "shallow crustal arrivals") that are tangent to Horizon B (labeled "top of oceanic crust") are clearly visible between 5-8 km and continuous with refracted first arrivals observed beyond 30 km range. Shallower high-velocity first arrivals are not observed in contrast to those revealed in sonobuoys 8 and 18 in the EMB (Figure 14).

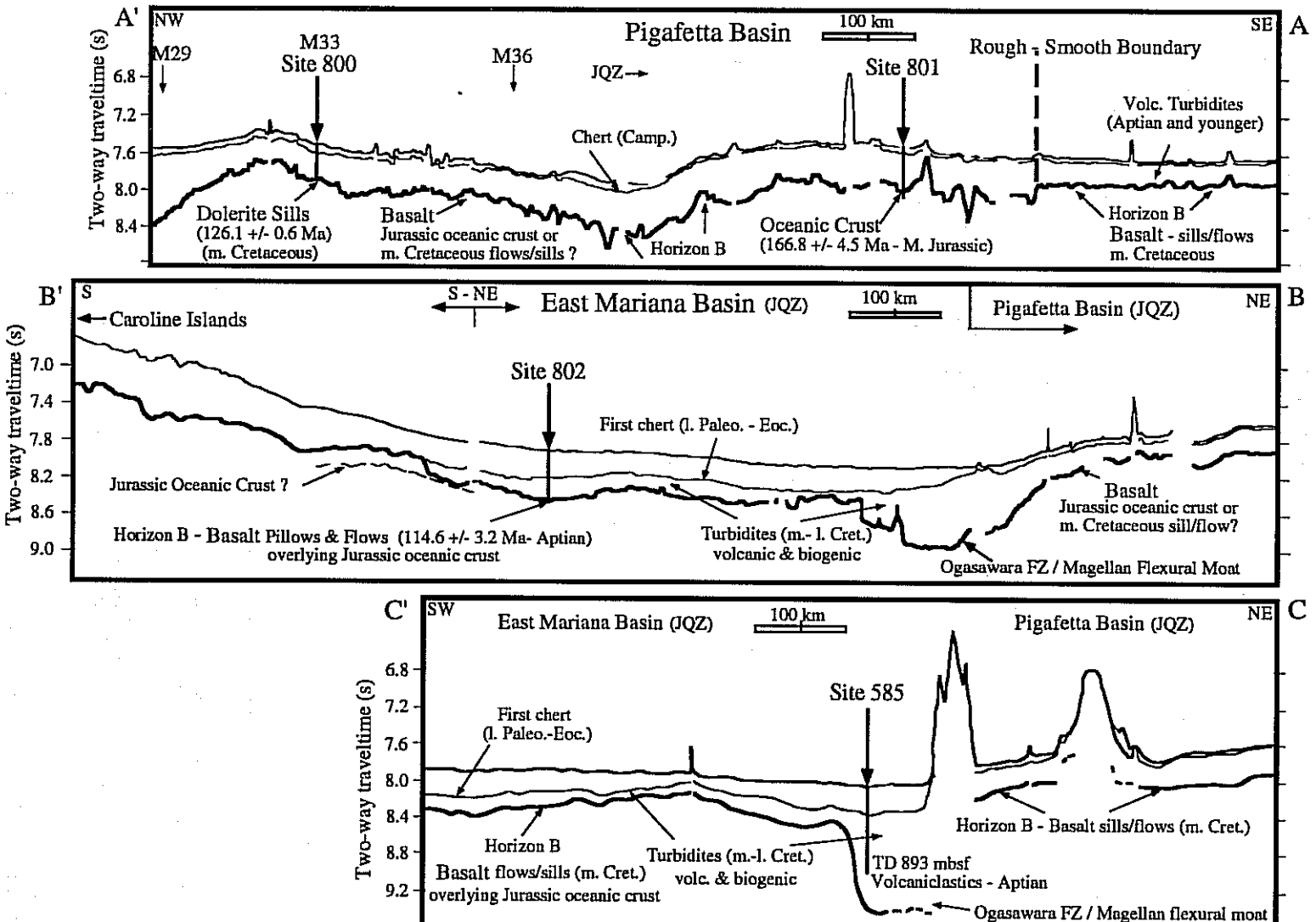

Fig. 6a-c . Three 900 - 1300-km long profiles showing selected reflections digitized from MCS airgun and near-channel watergun data (see Figure 4 track chart for locations (a) A-A', (b) B-B' and (c) C-C'). The deepest horizon (heavy line) represents the top of high-velocity igneous material. This horizon is characterized and interpreted from direct sampling at three widely separated ODP sites, reflection character and from velocity structure. The middle horizon represents the top of the shallowest chert - porcellanite - silicified limestone (First chert). The top horizon represents the seafloor. Note the depth difference between the PB and EMB, the deepening of Horizon B associated with the Ogasawara Fracture Zone and flexural moat of the Magellan Seamounts and the uniformly flat Horizon B surface (even at VE=133X) in the EMB and southeast PB compared to the high-relief basement of the PB northwest of the rough-smooth boundary. Radiometric ages are from Pringle [1992a].

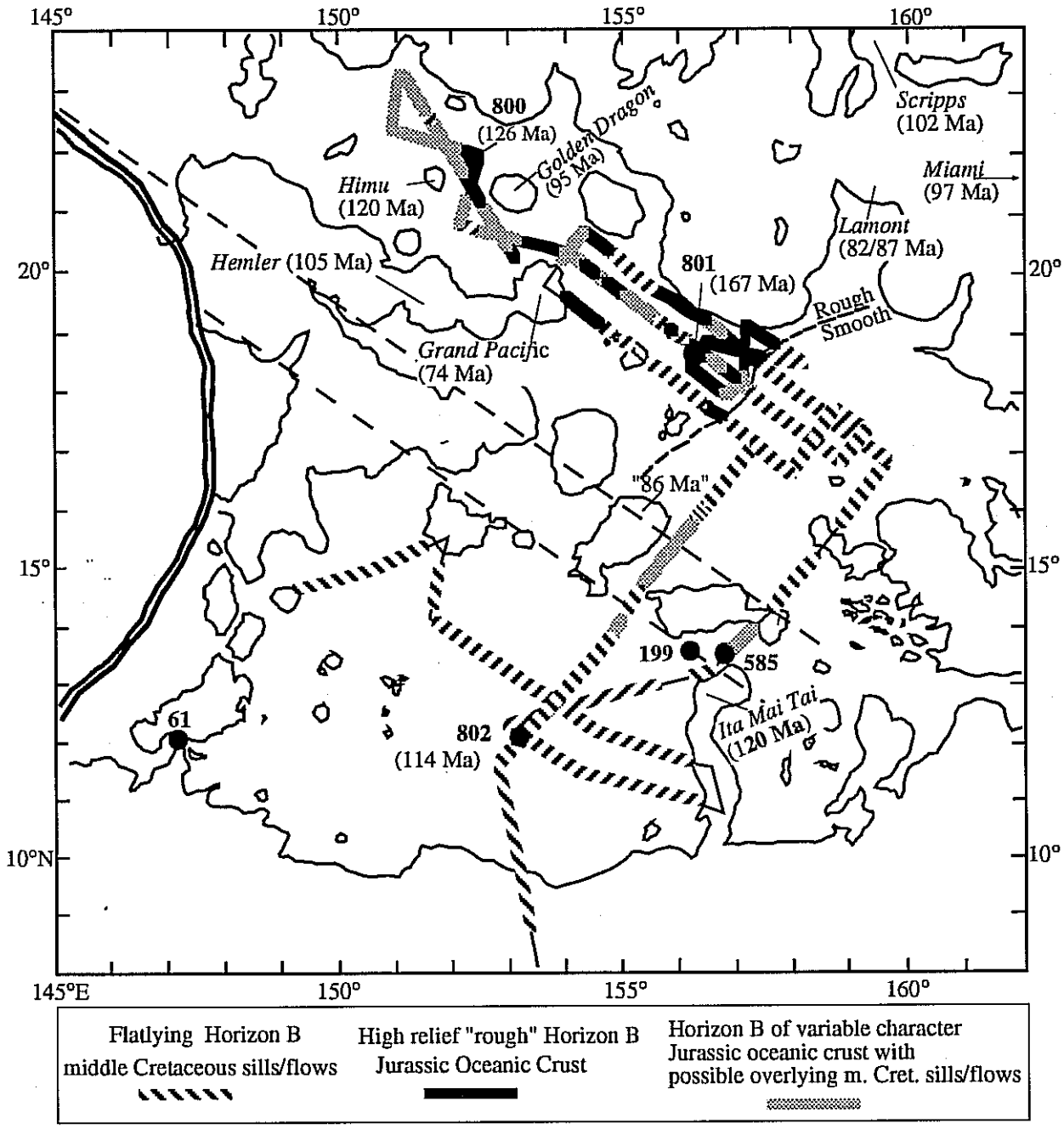

Fig. 7. Simplified bathymetry (5500 m contour is shown) of the central western Pacific modified from Brenner and Angell, [1992]. The reflection character of Horizon B and its interpretation are indicated along track from Abrams et al. [1992]. The oceanic crust in the entire EMB and southeast PB (~ 500,000 km^2) is overlain by mid-Cretaceous sills/flows (l. Barremian or younger). Only a few restricted areas in the PB are confidently interpreted to contain Jurassic oceanic crust with no massive igneous overburden. Horizon B in extended areas (primarily in the PB) is more tentatively interpreted as Jurassic oceanic crust with mid-Cretaceous sill/flow overburden possible. Radiometric ages of basalt are given in Ma for Leg 129 Sites from Pringle [1992a], and for seamounts from Ozima et al. [1983], Pringle [1992b], and Winterer et al., [this volume].

General Characterization of Horizon B

Horizon B is associated with the onset of high velocities (>3.6 km/s), and we believe it is often comparable in acoustic character to the unusually smooth basement observed in parts of the western North Atlantic and Caribbean Basin that was designated as Horizon B" [Ewing et al., 1967; Edgar and Saunders et al., 1973; Houtz and Ludwig, 1977]. Its reflection character and stratigraphic position determines whether

Horizon B is interpreted as the top of sills/flows overprinting true oceanic crust, or as Jurassic oceanic crust with no such massive igneous overburden.

In general, Horizon B can be characterized by two end-members: 1) a relatively high-relief, (50-100 m over tens of kilometers), lower reflection amplitude, diffractive ("rough") surface which always appears as acoustic basement and is interpreted as the top of oceanic crust, and 2) a flat-lying, high reflection amplitude, semicontinuous surface which often appears nondiffractive ("smooth"), does not necessarily appear as acoustic basement and is interpreted as sills/flows that overlie oceanic crust. A map view of the acoustic character of Horizon B and its interpretation is presented along seismic track lines in Figure 7. Figure 7 indicates that there are extensive areas in the northwest PB where the acoustic character does not clearly fall within the above-defined modes and/or these end-member characteristics alternate over distances of only tens of kilometers and as a result these areas have been more tentatively interpreted as the top of oceanic crust with possible sill/flow overburden.

Horizon B in The East Mariana Basin

In the majority of the EMB, Horizon B (heavy line in Figure 6) is high-amplitude, flat-lying, continuous and "smooth" (e.g. end-member 2). There are, however, several significant variations in its character. In restricted areas of the EMB

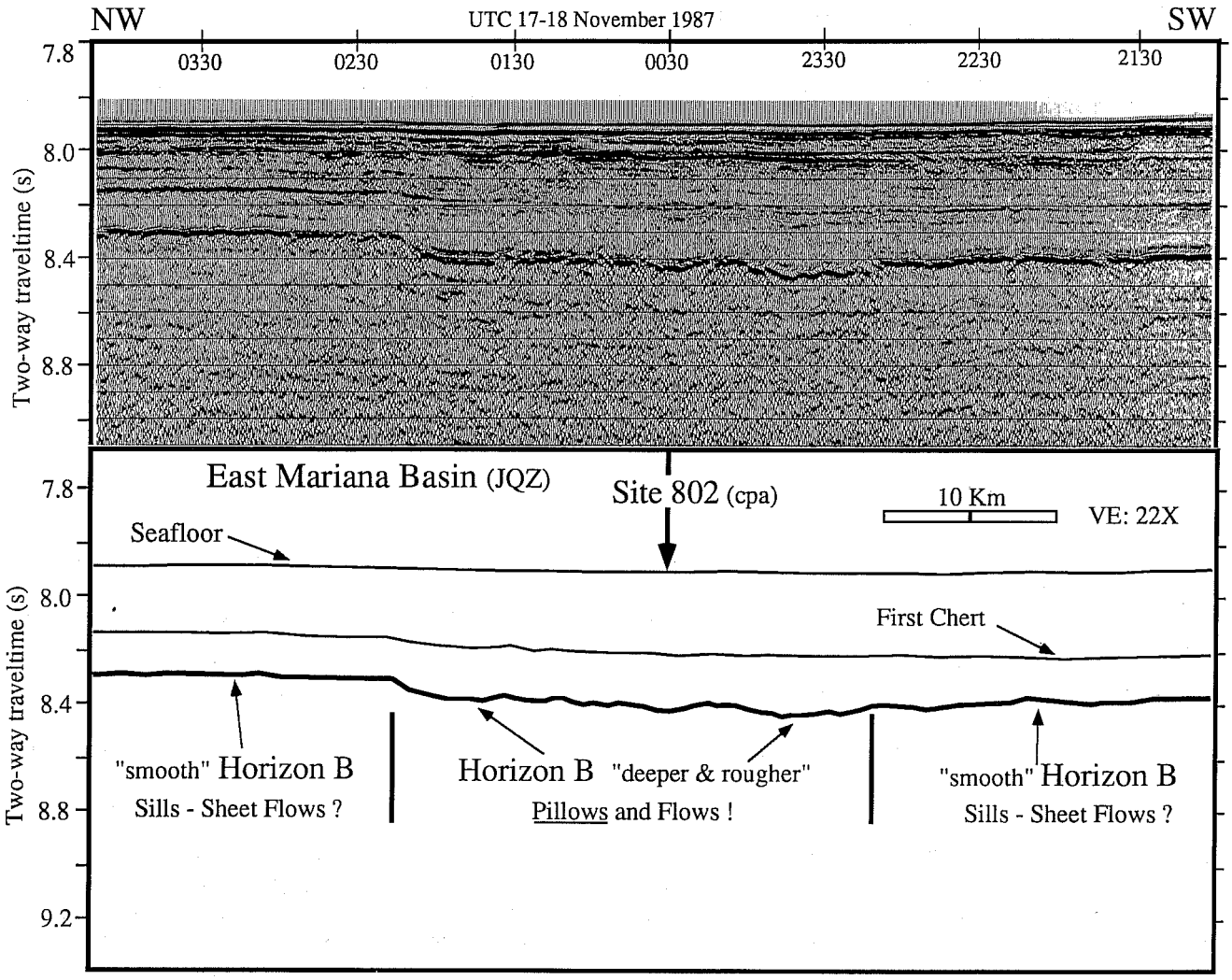

Fig. 8. FM35-12 MCS airgun profile at its closest point of approach (cpa) to Site 802 (approximately 4 km to the east). The depth and character of the basement reflector changes from a flat-lying, "smooth" event at 8.3 stwt to a "rougher" reflection at 8.4 stwt (marked by vertical lines). The "rough" (diffractive) Horizon B reflection correlates to the top of extrusive basalt (pillow units) and the shallow, "smooth" (non-diffractive) Horizon B reflection is interpreted as igneous intrusives or sheet flows. The relatively rough surface, however, remains flat-lying and shows much less overall relief than does the Horizon B in the PB northwest of the rough/smooth boundary. The processing and display parameters are as follows: pre-stack spike deconvolution, 120-fold stack, band-pass 20-60 filter Hz, F/K migration, 500 msec AGC and vertical exaggeration of ~22X at 1.5 km/s.

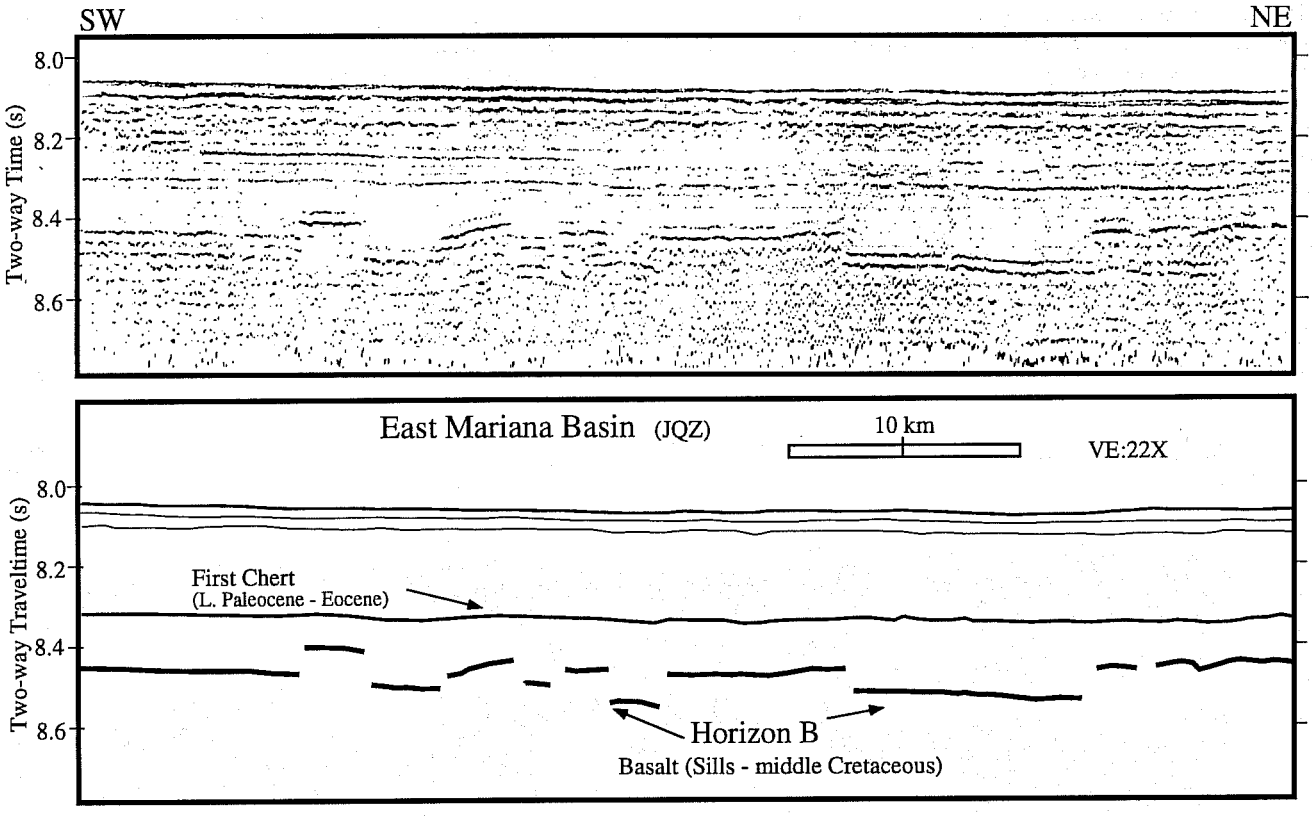

Fig. 9. MESOPAC II line 18 near-channel watergun profile in the EMB (location Figure 4) showing Horizon B where it appears flat-lying, "smooth" and laterally discontinuous "slablike". This type of reflection geometry is not characteristic of the top of oceanic crust and is interpreted as sills emplaced at different stratigraphic levels overlying an unimaged oceanic crust. This seismic record is processed and displayed as indicated in Figure 3.

Horizon B deepens slightly and becomes noticeably more diffractive (but still flat-lying), for example, at Site 802 where Horizon B corresponds to pillow and flow basalt (Figure 3c and 8). In other instances Horizon B appears to be divided by and contiguous with zones of poor reflectivity giving the appearance of "windows" through this ubiquitous horizon. A similar geometry is evident along the eastern EMB margin where Horizon B appears as a series of slabs which are offset laterally as well as vertically with no corresponding offset of the overlying sediment (Figure 9). To the south of Site 802, Horizon B appears continuous as it rises gradually from 6000 m to the 5000 m contour which marks the base of the Caroline seamounts, atolls and guyots (Figures 2, 10). The continuity of the gently rising Horizon B is only disrupted near the base of the Caroline Ridge by an offset (150 msec) which is not matched by offsets in the overlying reflections.

Two seismic profiles crossing the eastern margin of the EMB (Figures 6b and 6c) reveal the deepening of Horizon B from approximately 300-500 mbsf (8.3-8.5 stwt) to the west within the EMB to over 1150 mbsf (> 9.2 stwt) where the southern profile crosses DSDP Site 585. Correlations of seismic stratigraphy with drilling results from Site 585 indicate that the total depth reached at this site corresponds to a zone of relatively high-amplitude conformable reflections at approximately 8.9 to 9.0 stwt [Moberly and Schlanger et al., 1986, Abrams et al., 1992] and may correlate with the well-cemented, Aptian volcaniclastic turbidites and debris flows lying approximately 260 m above the high-velocity basement at 9.2 stwt as determined by sonobuoy 20 (Figure 11a). In this area there is no well-developed flat-lying, high-amplitude Horizon B observed. Finally, there are also sub-Horizon B reflection events observed in certain areas of the EMB. The suppression of bubble pulse multiples from Horizon B on processed FM35-12 MCS data revealed weaker, discontinuous reflections approximately 100 - 150 ms below Horizon B. The identification of these weak reflections, which are often identical in shape to the overlying Horizon B, as primary reflection interfaces rather than bubble pulse or interbed multiples is strengthened by isolated instances where these weak reflections display significant relief independent of flat-lying Horizon B and overlying sediments. A clear example of this type of reflection geometry is displayed in Figure 10.

The flat-lying, typically smooth character of Horizon B in the EMB and southeastern PB does not appear to change from profiles shot perpendicular to those shot parallel to magnetic lineations. This indicates that any abyssal hill morphology is

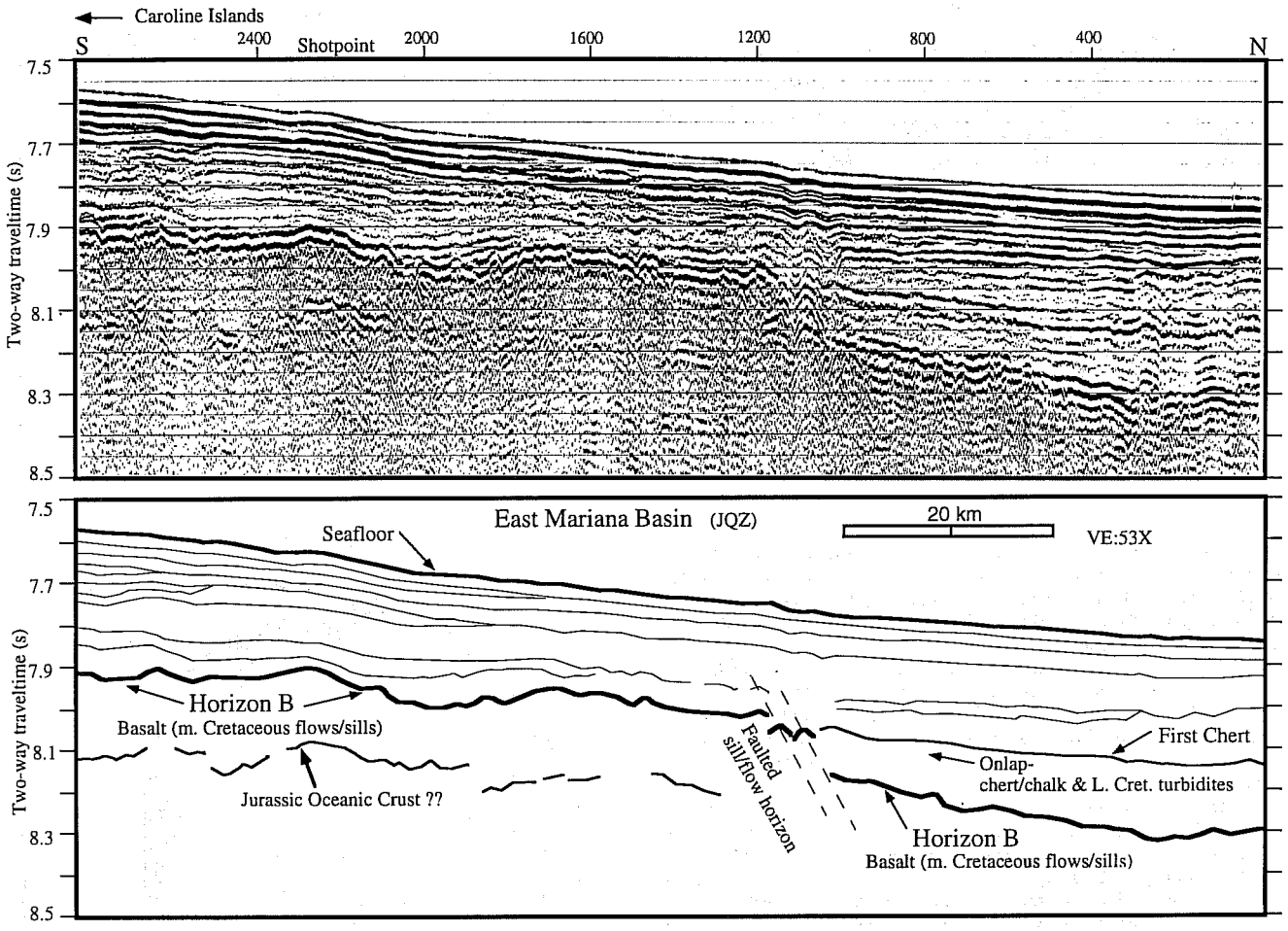

Fig. 10. MESOPAC II SCS watergun profile in the southern EMB (location Figure 4). Site 802 penetrated extrusive basalt dated at 114 +/- 3.2 m.y. beneath Aptian sediment, this horizon (Horizon B) appears faulted and is onlapped by late Paleocene chert/chalks and underlying Late Cretaceous turbidites. The basalt surface penetrated at Site 802 continues up onto the Caroline Ridge. A weak semicontinuous, relatively high-relief horizon imaged beneath the rising flow/sill surface is interpreted as the top of oceanic crust. A similar reflection geometry is observed on both airgun and watergun records in other restricted portions of the EMB. This MESOPAC II watergun record is processed and displayed as indicated in Figure 3.

muted, absent or buried and suggests that this is not the upper surface of oceanic crust. In addition, the Aptian age (124.5-112 Ma) of sediment overlying ~114 m.y. old extrusive basalt is approximately 50 m.y. younger than predicted from magnetic lineation correlations which had so successfully predicted the basement age at Site 801 (e.g. ~167 Ma) [Tamaki et al., 1987; Lancelot and Larson et al., 1990; Pringle, 1992a]. Thus, throughout the EMB, including the Caroline Ridge, Horizon B is interpreted as the top of middle Cretaceous flows and/or sills (probably late Barremian - Aptian) which overlie Jurassic oceanic crust. The weak sub-Horizon B reflections, though not penetrated at ODP Site 802, are interpreted as the top of oceanic crust.

Horizon B in The Pigafetta Basin

In the southeastern PB, Horizon B is semicontinuous, flat-lying and shallow (250-300 mbsf, 7.9-8.0 stwt). It is observed to monotonically deepen (400-480 mbsf) to the northwest becoming distinctly more diffractive (rougher), undulating, and lower in reflection amplitude beginning approximately 130 km southeast of, and including ODP Site 801 (Figures 6a and 12). This change in acoustic character from flat-lying to high-relief appears as a distinct boundary rather than an extended transition zone on our southeast to northwest seismic profiles and is designated as the "rough/smooth boundary" (Figures 4, 7 and 12). This boundary was located along profiles running southeast to northwest where flat-lying, semicontinuous Horizon B is first disrupted by a distinctly higher relief (perhaps tectonized) surface. To the northwest of the rough/smooth boundary, Horizon B displays a variety of reflection characteristics, which are superimposed upon a subtle, longer wavelength Horizon B surface (Figure 6a). Horizon B at Site 801 appears as a rough, undulating horizon that results primarily from a

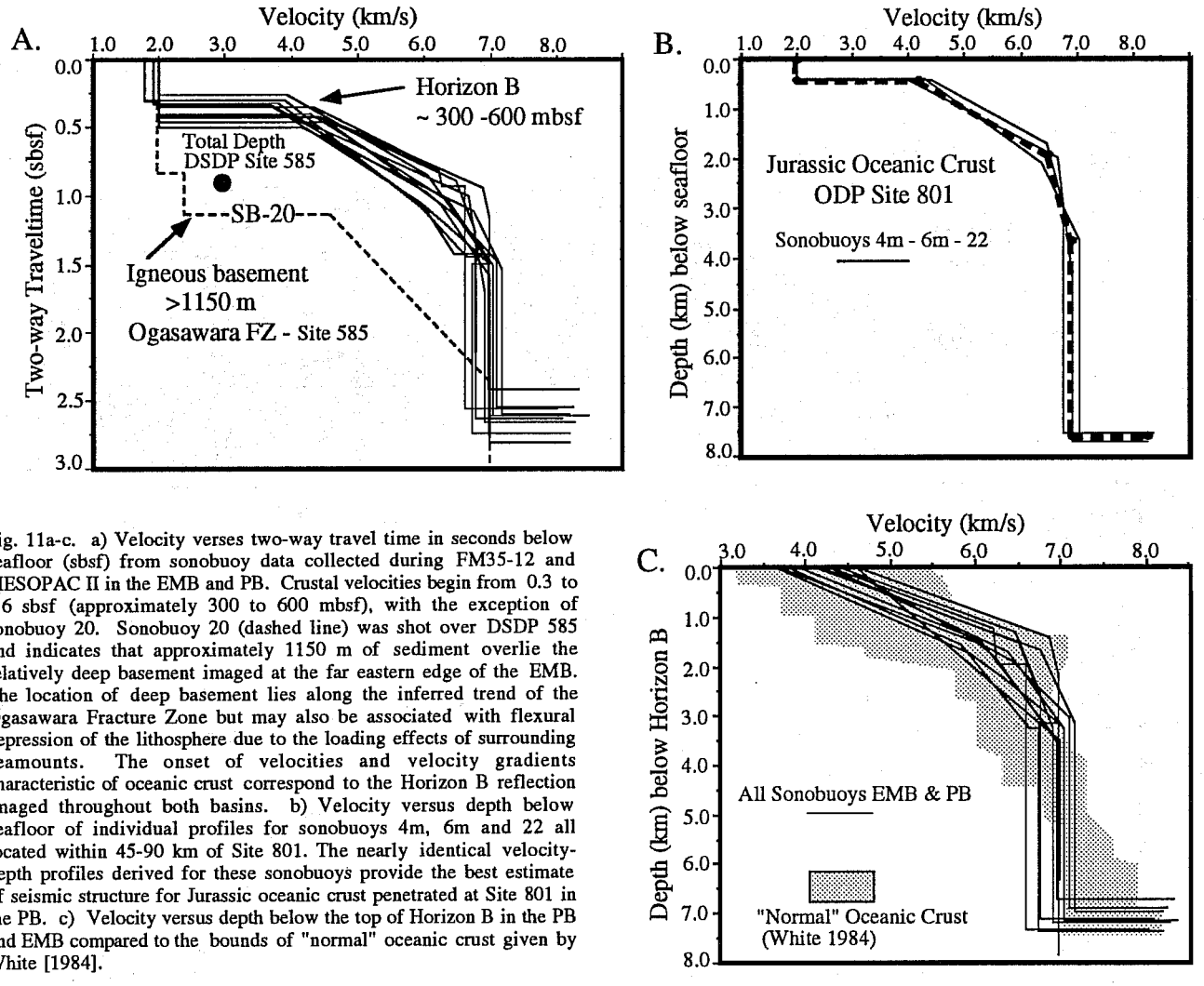

Fig. 11a-c. a) Velocity verses two-way travel time in seconds below seafloor (sbsf) from sonobuoy data collected during FM35-12 and MESOPAC II in the EMB and PB. Crustal velocities begin from 0.3 to 0.6 sbsf (approximately 300 to 600 mbsf), with the exception of sonobuoy 20. Sonobuoy 20 (dashed line) was shot over DSDP 585 and indicates that approximately 1150 m of sediment overlie the relatively deep basement imaged at the far eastern edge of the EMB. The location of deep basement lies along the inferred trend of the Ogasawara Fracture Zone but may also be associated with flexural depression of the lithosphere due to the loading effects of surrounding seamounts. The onset of velocities and velocity gradients characteristic of oceanic crust correspond to the Horizon B reflection imaged throughout both basins. b) Velocity versus depth below seafloor of individual profiles for sonobuoys 4m, 6m and 22 all located within 45-90 km of Site 801. The nearly identical velocity-depth profiles derived for these sonobuoys provide the best estimate of seismic structure for Jurassic oceanic crust penetrated at Site 801 in the PB. c) Velocity versus depth below the top of Horizon B in the PB and EMB compared to the bounds of "normal" oceanic crust given by White [1984].

large impedance contrast between the Callovian/Bathonian radiolarite clays and the top of interbedded chert/basalt and hydrothermal deposits which unquestionably represent the top of Jurassic oceanic crust (Figure 3b) [Lancelot and Larson et al., 1990]. In the areas to the southeast of Site 801 where Horizon B becomes flat-lying, "smooth" and shallow, and the overlying seismically transparent layer thins, sills and/or flows that are significantly younger (probably late Barremian - Aptian) than those recovered at Site 801 are expected to overlie oceanic crust (Figures 7 and 12 right side). Further to the northwest, Horizon B appears tectonized, sometimes exhibiting smooth, block faulted slabs having an apparent dip to the northwest.

Within the area of correlated magnetic lineations M29-M36 (Figures 1 and 2), Horizon B rarely appears similar to the rough, undulating basement horizon observed in the vicinity of ODP Site 801 (Figures 3b and 12 left side), however, it is not characterized by the extended areas of flat-lying, high-amplitude and "smooth" reflections observed in the southeast PB and the majority of the EMB. Specifically, there are no examples where Horizon B appears discontinuous and/or vertically offset as in the EMB (e.g. Figure 9). Horizon B at Site 800 correlates to the top of dolerite sills intruding Berriasian age [140-145 Ma] radiolarite clays. Although drilling at Site 800 penetrated through a thick middle Cretaceous volcaniclastic sediment unit and reached earliest Cretaceous pelagic sediments, Horizon B here does not represent oceanic crust because of the age (~126 Ma, Pringle, 1992a), thickness and obvious intrusive character of the dolerite, and because the oldest sediments would be expected to be Oxfordian in age (~160 Ma, M33).

The Horizon B reflections can be followed over the 550 km separating Sites 800 and 801. Results from these sites suggest that this horizon corresponds to the top of Jurassic oceanic crust where it appears particularly high-relief, undulating, lower in reflection amplitude, and diffractive. It corresponds to a thin, (approximately 100-400 m) middle Cretaceous igneous unit overlying oceanic crust where it appears flat,

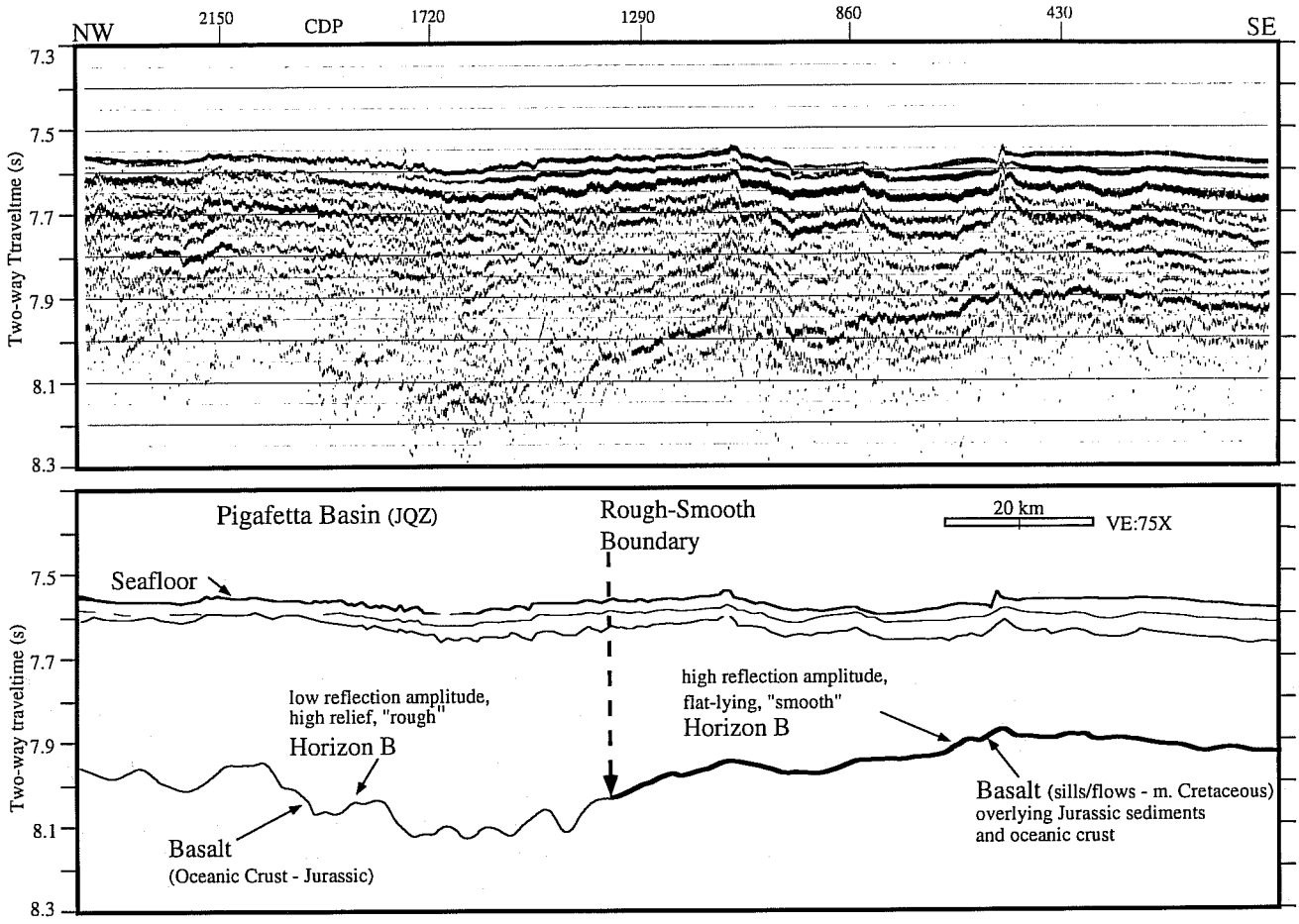

Fig. 12. FM35-12 MCS airgun profile in the JQZ of the PB along an inferred flowline course and displayed at true relative amplitude. The continuous, flat-lying (at VE:75x) and high-amplitude Horizon B reflection southeast of the rough/smooth boundary deepens and appears to be contiguous with an undulating, diffractive and lower reflection amplitude "rough" Horizon B. The "rough" Horizon B correlates to the top of middle Jurassic oceanic crust (e.g. Site 801) and the "smooth" horizon is interpreted as mid-Cretaceous sills and flows overlying the unimaged top of oceanic crust. The rough/smooth boundary appears on all five of our tracks crossing this area and a comparable boundary is not apparent in the EMB. We suggest that the boundary marks the limit of semicontinuous mid-Cretaceous (Aptian?) flows/sills. The processing and display parameters are the same as in Figure 8 except displayed with true relative amplitude, band-pass filter 8-25 Hz and vertical exaggeration of ~75X at 1.5 km/s.

high-amplitude, "smooth" and slablike. The actual thickness of the middle Cretaceous sills and flows, however, is uncertain, and aspects of this determination are discussed in the following section.

Sill/Flow/Sediment Thickness

To establish the relationship between Horizon B and the top of oceanic crust by focusing on evidence for sills/flows overlying oceanic layer 2, we first describe the area in the PB where Horizon B correlates to the top of Jurassic oceanic crust. We then compare the velocity-depth profiles and record sections from this area to areas in the PB and EMB where Horizon B correlates to the top of middle Cretaceous sills and/or flows.

In Figure 11 and Table 1 we show Vp versus depth functions obtained from 13 sonobuoys. The velocity-depth functions below the seafloor are given in terms of a series of constant velocity gradient layers. Figure 11a indicates that velocities and/or velocity gradients characteristic of oceanic crust begin at or just below the dominant Horizon B reflection, imaged regionally at 300 to 600 mbsf. Sonobuoy 20, shot over DSDP Site 585, is the one exception to this relationship and indicates that approximately 1150 m of sediment overlie high-velocity basement in the area that we identify as the Ogasawara Fracture Zone (Figures 2, 6).

Sonobuoys 4m, 6m and 22 (Figures 5 and 11b) within 45-95 km of ODP Site 801 provide the best constraints on crustal structure, not only because a complete suite of arrivals are

Table 1. Velocity - Depth functions below seafloor given in terms of a combination of constant velocity gradient layers with top and bottom velocities for each layer given in column 3. Dashes indicate constant velocity layer. The thickness of each layer given in seconds (s) and kilometers (km) (column 4). Velocity gradient (s-1) for each layer is given in column 5.

SB#	Layer	Water Depth (m)	Vp (km/s)	Thickness (s) - (km)		Gradient (s -1)
4m	1	5730	2.0 -	.42	.42	0.0
	2		4.41-6.47	.47	1.28	1.61
	3		6.47-6.76	.38	1.24	0.23
	4		6.76 -	1.36	4.59	0.0
6m	1	5660	2.0 -	.40	.40	0.0
	2		4.15-6.38	.64	1.69	1.32
	3		6.38-7.03	.46	1.54	0.42
	4		7.03 -	1.10	3.89	0.0
22	1	5680	2.0 -	.41	.41	0.0
	2		3.98-6.67	.59	1.58	1.71
	3		6.67-6.92	.70	2.38	0.11
	4		6.92 -	.96	3.33	0.0
1m	1	5585	2.0 -	.50	.50	0.0
	2		4.13-6.75	.61	1.65	1.58
	3		6.75-7.17	.43	1.48	0.28
	4		7.17 -	1.06	3.82	0.0
2m	1	5680	2.0 -	.46	.46	0.0
	2		4.63-6.87	.49	1.41	1.59
	3		6.87-6.98	.22	0.75	0.15
	4		6.98 -	1.44	5.03	0.0
3m	1	5755	2.0 -	.35	.35	0.0
	2		4.32-6.21	.47	1.23	1.54
	3		6.21-6.26	.12	0.73	0.07
	4		6.6 -	1.62	5.36	0.0
23	1	5660	2.0 -	.43	.43	0.0
	2		4.45-6.43	.69	1.87	1.06
	3		6.43-7.09	.35	1.17	0.57
	4		7.09 -	1.08	3.83	0.0
8m	1	5745	2.0 -	.34	.34	0.0
	2		3.70-6.03	.63	1.52	1.53
	3		6.03-6.24	.09	0.29	0.73
	4		6.24-6.98	.53	1.74	0.42
	5		6.98-	1.16	4.27	0.0
21	1	5685	2.0 -	.26	.26	0.0
	2		3.92-6.06	.59	1.46	1.46
	3		6.06-6.96	.62	2.01	0.45
	4		6.96 -	.95	3.25	0.0
20	1	6100	1.8 - 1.8	.30	.27	0.0
	2		2.0 - 2.0	.52	0.52	0.0
	3		2.4 - 2.4	.30	0.36	0.0
	4		4.60-7.00	1.23	3.50	0.68
	5		7.00-	.80	2.80	0.0
7	1	5925	1.9 -	.32	.30	0.0
	2		3.81-5.83	.70	1.69	1.2
	3		5.83-6.63	.42	1.31	0.61
	4		6.77 -	.70	2.37	0.0
8	1	5940	1.9 -	.33	.32	0.0
	2		3.66-5.94	.72	1.73	1.32
	3		5.94-6.33	.16	0.49	0.8
	4		6.33-6.98	.28	0.93	0.7
	5		6.73-	1.25	4.19	0.0
18	1	5930	1.78 -	.30	.27	0.0
	2		3.90-6.04	.82	2.04	1.05
	3		6.04-6.45	.3	0.92	0.44
	4		6.98 -	1.39	4.86	0.0

Table 2. Layer 2 thicknesses as defined by velocity and velocity gradient, and total crustal thicknesses are given. Mantle arrivals were not observed for sonobuoy 7 (SB7).

SB#	Layer 2 Thickness (km) (<6.4 km/s) - (1-2 s-1)		Total Crustal Thickness (km)
4m	1.3	1.3	7.12
6m	1.7	1.7	7.12
22	1.42	1.58	7.28
1m	1.44	1.65	6.95
2m	1.11	1.41	7.18
3m	1.96	1.23	7.31
23	1.84	1.87	6.86
8m	1.90	1.52	7.83
21	2.22	1.46	6.76
20	2.61	–	6.35
7	2.6	1.7	–
8	2.32	1.73	7.34
18	2.85	2.04	7.82

observed, but also because Site 801 is the single location where Jurassic oceanic crust undoubtedly exists without any younger igneous overburden. Velocity-depth functions of these three sonobuoys are shown separately in Figure 11b. The normal-incidence two-way reflection time through this structure agrees to better than 0.1 s with the location of the Moho reflection observed on FM35-12 MCS profiles collected during the acquisition of sonobuoy 22 (Figure 13). The total crustal thickness is 7.2 km (2.22 stwt), overlain by an average 410 m of sediment. The remaining sonobuoys are divided into groups representative of distinct areas of the EMB and PB (Figures 2 and 4 location). Layer thicknesses derived from these sonobuoys are defined and listed in Table 2.

Analysis of T/X data along with the drilling results from ODP Sites 800, 801 and 802 clearly establish that Horizon B represents the top of high-velocity (>3.6 km/s), massive igneous material throughout these basins. The greatest limitation of this travel time-range study is that in those cases where short range refracted second arrivals in the critical range (5-8 km) are obscured by seafloor and Horizon B reflections it is impossible to distinguish between a variety of probable velocity structures (resolvable at seismic wavelengths) between the Horizon B reflection and the structure revealed by longer range (deeper) refracted arrivals. The necessity of assuming or calculating a velocity for the uppermost crust (layer 2a, b or in this case the layer beneath Horizon B) because of the lack of observable refracted arrivals is well documented [Ewing and Purdy 1982]. The problem here is that other evidence indicates that sills/flows and sediment actually overlie Jurassic oceanic crust (layer 2) in the majority of the EMB, and in the PB southeast of the rough-smooth boundary. Modeling the structure immediately below Horizon B as a single velocity gradient in these areas of the EMB and PB in effect includes middle Cretaceous sills/flows and sediments as part of layer 2.

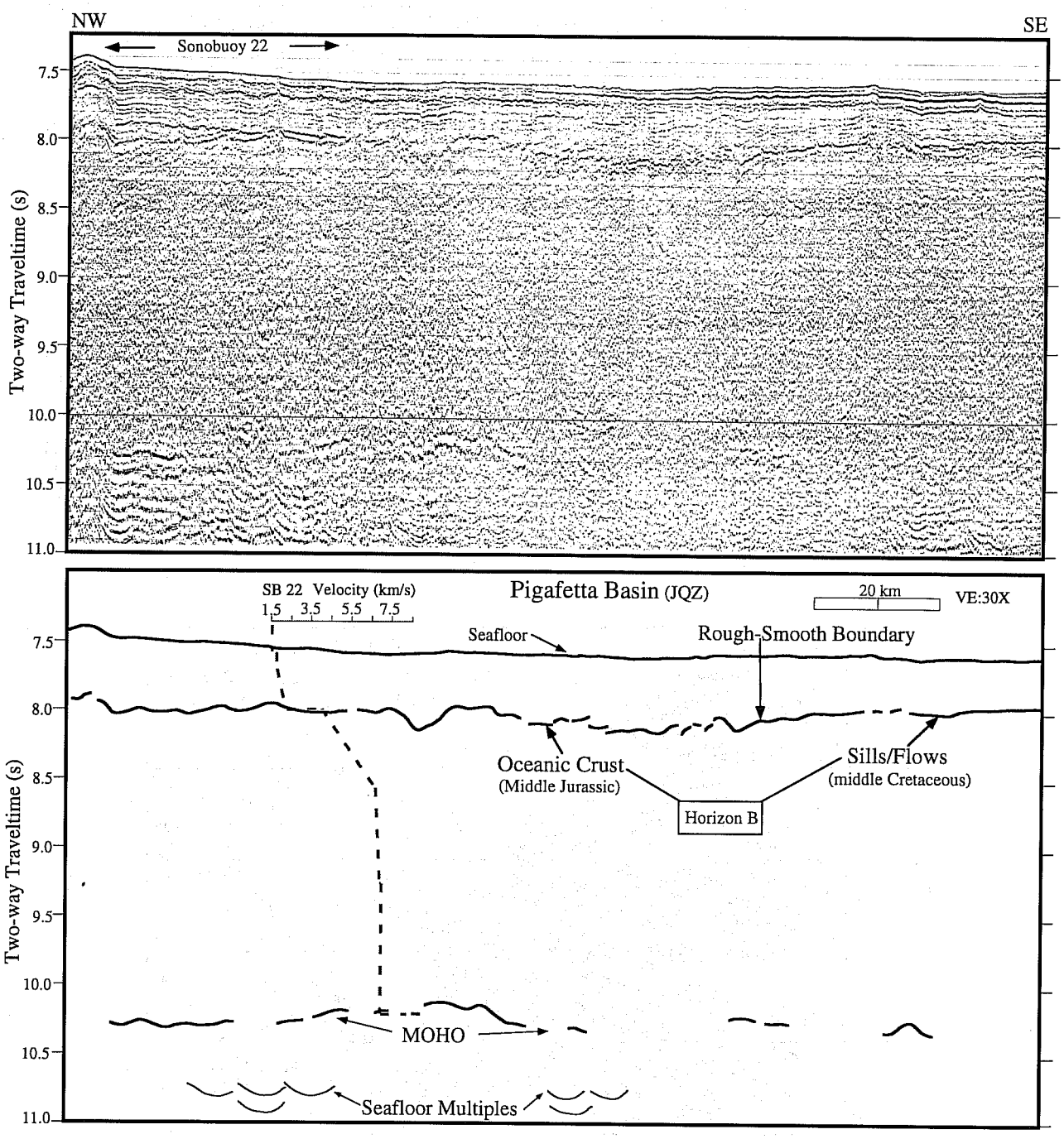

Fig. 13. FM35-12 MCS airgun profile in the JQZ of the PB with the velocity-depth profile derived from sonobuoy 22 superimposed. The onset of velocities and velocity gradients characteristic of oceanic crust correspond to the Horizon B reflection. Sonobuoy 22, 6m and 4m all located within 45-90 km of Site 801 provide nearly identical velocity-depth profiles including wide-angle mantle reflections with intercept times matching those observed in the MCS profile labeled MOHO at ~10.2 stwt. Processing and display parameters are the same as in Figure 8 except band-pass filter 8-25 Hz and vertical exaggeration of ~30X at 1.5 km/s.

Velocity-depth structures calculated in this way fall within the wide bounds defining normal oceanic crust (Figure 11c; Houtz and Ewing, 1976; Spudich and Orcutt, 1980; White, 1984) and total crustal thicknesses do not appear significantly different between the EMB and PB (Table 2). Assuming layer 2 thicknesses determined from sonobuoys 22, 4m and 6m are representative of Jurassic oceanic crust in this area implies that the middle Cretaceous sill/flow/sediment complex in the

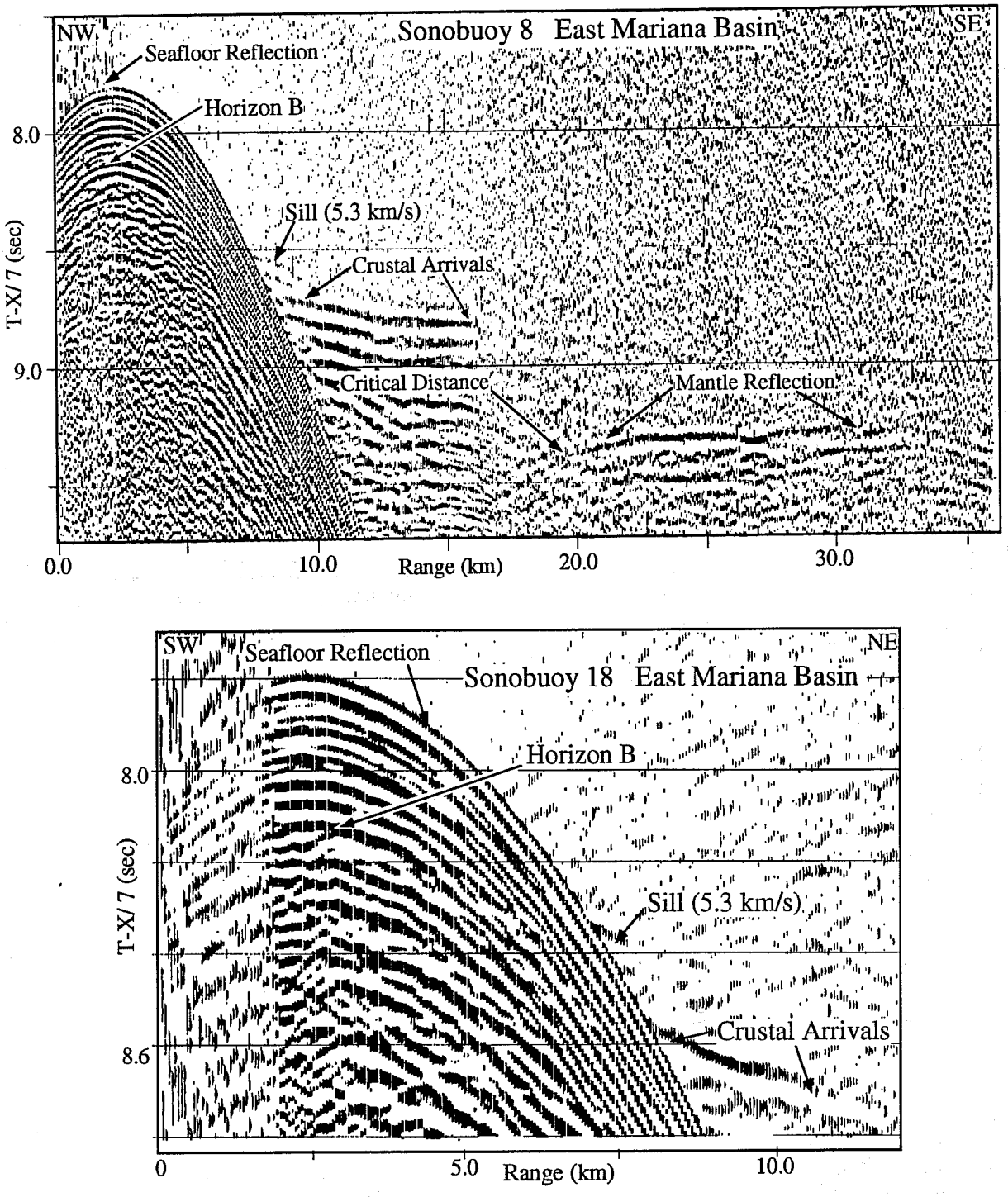

Fig. 14a-b. a) Sonobuoy 8 in the JQZ of the EMB located 120 km North of Site 802 is shown over the entire range of the sonobuoy (>35 km). b) Sonobuoy 18 in the JQZ of the EMB located 130 km northeast of Site 802 is shown over 0-15 km range. Note the lower amplitude, shallow first refracted arrival with a phase velocity of 5.3 km/s (labeled "sill") which appears tangent to the Horizon B reflection (SB18) or to reflections just below Horizon B (SB8). This short range arrival is indicative of a high-velocity layer (sill/flow) overlying lower velocity sediment and oceanic crust. Similar arrivals are not observed on sonobuoys northwest of the rough/smooth boundary (compare to Figure 5). Sonobuoy data displayed at reduced travel time (7km/s), band-pass filter 8-25 Hz.

EMB may range in thickness from 0 to approximately 1 km depending on how layer 2 is defined (e.g. Table 2, 1.7 to 2.85 km vs 1.3 to 1.7 km). Thus, there is no seismically resolvable, systematic differences in crustal velocities and thicknesses between areas where middle Cretaceous sills/flows are present and where they are absent. This observation is significant when compared to anomalously thick crust observed in portions of other basins where a smooth basement reflection (Horizon B or B") corresponds to the surface of younger (middle to Late Cretaceous) sills/flows throughout an area predicted to contain Jurassic sediment and oceanic crust such as the Nauru Basin (Figure 1) and basins of the Caribbean Sea [Edgar and Saunders et al., 1973; Larson and Schlanger et al., 1981; Wipperman et al., 1981; Diebold et al., 1981].

The results from sonobuoys in the EMB, however, provide further support for the presence of sills/flows overlying sediment and oceanic crust. In two instances (sonobuoys 8 and 18) low-amplitude refracted arrivals of limited range appear tangent to or slightly below the Horizon B reflection (Figure 14a,b, arrival labeled "sill"). These weak but distinct events extend as first arrivals that overlie the higher amplitude, continuous refractions that characterize normal oceanic crust. These arrivals have a phase velocity of approximately 5.3 km/s and show a rapid decay in amplitude with range. Such observations are consistent with the existence of a high-velocity igneous layer capping lower velocity sediments which overlie oceanic crust. Shallow "sill" refractions are not observed on any sonobuoy records from the PB (e.g., Sites 800 and 801; compare Figures 5b and 14b). We note that the velocity-depth solutions given in Table 1 were derived by matching the stronger, more coherent and longer range arrivals that occur approximately 0.15 sec below the weaker first arrivals labeled "sill". This was done primarily because ray theory cannot simultaneously match both sets of arrivals over the same range when the velocity of the shallow first arrival is greater than that of the deeper second arrival.

In order to be imaged as a separate unit, the sill/flow sediment complex must create an impedance contrast with layer 2 at least 1/4 of a seismic wavelength in thickness (> 50 - 125 m). If one is looking for a velocity discontinuity representing the base of sill/flow/sediment and top of layer 2 then the most appropriate factor to examine is the presence or absence of reflections. In the EMB, low-amplitude, discontinuous reflections observed 0.1-0.15 stwt below Horizon B may be due to the impedance contrast between Jurassic oceanic crust and pre-Aptian (>124.5 Ma) pelagic sediment with Aptian sills/ flows. The velocity at the top of this interval is approximately 5.3 km/s as revealed by weak, short-range refractions observed on sonobuoys in the EMB (Figure 14a,b) and approximately 5.8 km/s as determined by the average velocity of basalt samples from Site 802 [Lancelot and Larson et al. 1990]. Assuming an average velocity of 5.3 km/s for the interval between the top of Horizon B and top of the weak sub-Horizon B reflections (top of oceanic crust) results in a maximum thickness of 265-398 m for the Aptian flows/sills and interbedded sediment.

DISCUSSION

The thickness of middle Cretaceous igneous overburden and pre-middle Cretaceous sediments in the EMB and portions of the PB is estimated at 100 - 400 m based on the following corroborative evidence.

1) The similarities of upper crustal velocity structure and total crustal thicknesses derived from T/X sonobuoy data throughout the PB and EMB indicate a maximum thickness of approximately 1 km. However, based on weak sub-Horizon B reflections, the maximum thickness for this unit is better estimated at 400 m, as discussed above.

2) Synthetic seismograms created from a simplified impedance structure at Site 802, which employ the source waveform from FM35-12 and Mesopac II, indicate that a minimum sub-Horizon B layer thickness of 200 m can be resolved, that is the top of Horizon B and the top of oceanic crust appear as two separate reflection events. We interpret the discontinuous and low amplitude nature of reflections from the top of oceanic crust as due to the vertical resolution of the seismic signal and, to a lesser degree, the lack of seismic energy penetration resulting from the high reflection coefficient of Horizon B. In the majority of the EMB and PB the thickness of the sill/flow/sediment complex above oceanic crust is on the order of our ability to easily resolve seismically (e.g. ~200 m). When this layer thins, the already weak reflection from the top of oceanic crust merges with and becomes part of an interference pattern created by closely spaced impedance contrasts that begin with Horizon B. Furthermore, we expect that only 100 to 150 m of sediments are intruded and or capped by sills/flows at Sites 800 and 802, respectively, assuming that a sedimentary section comparable to Site 801 is representative of the PB and EMB for sediment deposited prior to the onset of middle Cretaceous volcanism.

3) The relatively high-relief, diffractive reflection associated with the top of oceanic crust at Site 801 is observed to extend semicontinuously to the northwest where the basement horizon alternates between rough, high-relief (e.g. Site 801) and relatively smooth and flat-lying (e.g. sills/flows) while remaining at the same depth. This type of reflection geometry is inconsistent with a widespread, thick overburden of igneous material.

In the EMB and PB middle Cretaceous sills/flows are identified along more than 4000 km of trackline throughout an area of approximately 500,000 km^2 (Figure 7). Assuming a maximum thickness of 500 m allows a volume estimate for deep sea middle Cretaceous sills/flows in the EMB/PB of ~0.25 x 10^6 km^3. Although arealy extensive, the estimated volume is small compared to volume estimates for well-known flood basalts such as the Deccan Traps (~2 x 10^6 km^3 - Courtillot et al., 1987) and to large oceanic plateaus such as Ontong-Java (~ 50 x 10^6 km^3 - Schubert and Sandwell, 1989).

Tectonic Setting and Source of Deep Sea Volcanism

The MCS coverage of the EMB and PB along with bathymetry provide additional constraints on the

morphotectonic expression of possible volcanic sources. The geometry of the "rough/smooth boundary" in the PB and the continuation of the middle Cretaceous igneous surface up onto the Caroline Ridge south of the EMB indicate that sources for these semicontinuous sills/flows extend to the south. Basalts recovered in the EMB are similar in age and in major, trace and isotopic element composition to basalts recovered in the Nauru Basin and the Ontong-Java Plateau (Figure 1), all showing strong affinities to MORB with a variably enriched mantle I (EM I) deep mantle source component [Castillo and Carlson, 1990; Mahoney and Tarduno, 1990; Castillo and Pringle, 1991; Tarduno et al., 1991]. These authors have speculated that the Nauru Basin and EMB were both sites of deep sea volcanism associated with the rapid formation of the Ontong-Java Plateau. Our seismic observations are consistent with this notion and indicate that the southeast PB was similarly affected. Northwest of the "rough/smooth boundary" (e.g., Sites 800 and 801) middle Cretaceous deep sea volcanism is much more restricted, being associated with individual seamounts and or seamount provinces as indicated by the comparable ages and distinct geochemistries of both the sills penetrated at Site 800 and samples dredged from Himu and Golden Dragon seamounts (Figures 2 and 7) [Smith et al., 1989; Castillo and Pringle, 1991, Pringle, 1992b; Castillo et al., 1992]. Continuity between these types of volcanic structures (seamounts, plateau, and deep sea flood basalts) is not observed seismically, so any inference of genetic relationships requires geochemical comparisons. However, the syncronicity in emplacement of these volcanic constructs with increased world-wide spreading rates (increased total crustal production) and the onset of the Cretaceous Normal Polarity Superchron (~124 Ma) is clear and may be the consequence of sudden heat and material transfer from the core/mantle boundary in the form of a rising plume resulting in excess mantle melt generation [Larson, 1991a,b].

The local volcanic sources and actual mode of emplacement of laterally extensive deep sea igneous provinces is still unknown. The most probable tectonically-controlled source location for middle Cretaceous volcanism is the Ogasawara Fracture Zone because of its association with large middle Cretaceous seamounts. Magnetic anomalies M22-M36 are offset approximately 500-600 km left-laterally from the EMB to the PB and are separated by a region approximately 300 km wide (Figure 2). The Ogasawara Fracture Zone that offsets these lineations lies somewhere within this broad zone, the two seismic profiles across this region indicate that the fracture zone lies along the northeastern margin of the EMB (e.g. southwestern dashed line in Figures 2, 4, and 7) where the depth to seafloor and to Horizon B is greatest (Figure 6). Seamounts of the Magellan Group are scattered within this region and appear to be aligned along the trend inferred for a fracture zone offset. Intra-plate volcanism in the form of volcanoes and elongate ridges that are localized along and within fracture zones is well documented and has been used as an argument for a weakened lithosphere along fracture zones [Vogt, 1974; Batiza, 1981; Lowrie et al., 1986]. The apparent alignment of the southern Magellan Seamounts along this fracture zone in addition to age constraints from dredge samples and cored volcanogenic material indicate that it became one of many focal points for mid-plate volcanism beginning in the Aptian and extending into the Santonian. The observation of the middle Cretaceous flow/sill unit (Horizon B) possibly onlapping Ita Mai Tai and another unnamed large guyot in the EMB, as well as the distinct isotopic signatures of both Himu seamount and the sills recovered at Site 800, indicate that these Aptian age seamounts may have acted as a local source for deep sea volcanism. The recovery of Aptian pillow basalt at Site 802, located more than 300 km from the most proximal seamount, and the huge areal extent of these basalts, indicate that individual seamounts are not the direct volcanic sources in the majority of the EMB and southeast PB.

Large seamounts of the Magellan Group, however, may provide another, more indirect, mechanism for deep sea lava flow emplacement. Lipman et al. [1989] and Clague et al. [1990] report the presence of widespread, young lava flows at several sites along the Hawaiian arch approximately 200 km from the island chain. These remarkably flat-lying areas of up to 25,000 km^2, which are characterized by high-acoustic backscatter and hyperbolic reflections on GLORIA and seismic reflection images respectively, correspond to young lava flows. The spatial association of sheet flows with the Hawaiian Flexural Arch, as well as with clusters of Cretaceous seamounts, led Clague et al. [1990] to speculate that lavas are derived from magma concentrated beneath the upbowed lithosphere of the flexural arch and delivered to the surface where the lithosphere locally responds to the seamount load by fracturing.

Individual flows may extend for 100 km, however, the vents for these extensive Hawaiian Arch sheetflows have not been identified, despite the lack of sediment cover [Clague et al., 1990]. Similarly, the morphotectonic expression of such vents, fissures or rifts (spreading or not) is not obvious in the available bathymetric maps or limited seismic profiles in the PB/EMB. In fact, it is difficult to detect tectonic fabric of any kind in the EMB or southeastern PB, most likely due to the masking effects of the pervasive flows and sills. The example of Hawaiian Arch flows also indicates that the seismic expression of potential vents and fissures can be quite subdued. However, the subtle, localized deepening and associated increase in roughness of Horizon B, which we have interpreted as pillow/flow units in the EMB, may represent such fissures and vents (Figure 8).

Magnetic Rough-Smooth Boundary

The distinctive change in the seismic character of Horizon B in the PB from "smooth" to "rough" can also be correlated to a change in magnetic anomaly amplitudes and field strength [Handschumacher et al., 1988]. The "rough/smooth" Horizon B boundary (Figure 4) is nearly coincident with the magnetic boundary interpretation of Handschumacher et al. [1988] which marks a change in magnetic anomalies from higher

field/lower-amplitude anomalies to lower field/higher-amplitude anomalies. A comparable seismic-magnetic boundary within the EMB, which is characterized by the nearly ubiquitous presence of the high-amplitude flat-lying Horizon B, is not apparent. Handschumacher et al. [1988] suggested that the distinct change in magnetic character in the PB may represent a change in spreading rate and/or direction, or a fossil plate boundary. We suggest an additional possibility, that both seismic and magnetic rough-smooth boundaries mark the geographic extent of continuous, middle Cretaceous, igneous overburden in the PB. If this is the case then the change in magnetic anomaly character at the "rough/smooth boundary" is due to the edge of normally magnetized Cretaceous sills/flows overlying and adjacent to mixed polarity Jurassic oceanic crust.

A similar seismic-magnetic "rough/smooth" boundary associated with the central Venezuelan Basin Fault Zone (CVF) in the Caribbean Sea has also been recognized. The CVF has been interpreted as marking the boundary between an anomalously thick Late Cretaceous igneous province built upon pre-existing oceanic crust and normal thickness oceanic crust [Talwani et al. 1977; Diebold et al., 1981]. While the crustal thickness variation across the "rough/smooth boundary" in the PB is not as large, there is also the possibility that this "boundary" may mark the location of a fracture zone (Mendocino?) offsetting the proto-Pacific/Farallon ridge [Handschumacher et al., 1988], which in middle Cretaceous time acted as a structural boundary to sills and flows originating from sources to the south.

CONCLUSIONS

1) Analysis of seismic travel time-range data along with drilling results from ODP Leg 129 clearly establish that Horizon B represents the top of high-velocity, massive igneous material throughout the EMB and PB. Horizon B displays a range of reflection characteristics between two end-member modes. It corresponds to the top of Jurassic oceanic crust where it has a high-relief, undulating, lower amplitude and diffractive character. It corresponds to middle Cretaceous sills/flows overlying oceanic crust where it appears flat-lying, high-amplitude, discontinuous and often "smooth". These Horizon B reflection characteristics calibrated by Leg 129 drill sites indicate that a semicontinuous sequence of middle Cretaceous deep sea flows/sills overlies Jurassic sediments and oceanic crust throughout an area of approximately 500,000 km^2 in the EMB and southeast PB.

2) Sonobuoy refraction data indicate no significant (> 1 km) difference in crustal thicknesses between areas overlain by documented middle Cretaceous sills/flows and areas with Jurassic oceanic crust free of such younger igneous overburden. Based on sub-Horizon B reflections and velocity information from sonobuoys, we estimate the maximum thickness of the middle Cretaceous sill/flow/sediment complex at 100 - 400 m. The volume of deep sea sills and flows in the EMB/PB is estimated at 0.25×10^6 km^3, approximately 200 times less than the volume estimated for the Ontong-Java Plateau.

3) A distinct smooth-to-rough Horizon B boundary is found in the southeast PB where the continuous overburden of middle Cretaceous flows/sills pinch out and expose Jurassic oceanic crust. Northwest of this boundary, occurrences of late Barremian - early Aptian sills/flows are documented, but are believed to be localized and associated with individual seamounts of similar age and isotopic character.

4) The change in magnetic anomaly character in the so called Jurassic Magnetic Quiet Zone of the PB from rough to smooth is associated with the change in reflection character of Horizon B from smooth to rough. This kind of magnetic and seismic boundary is not observed in the EMB, and it is believed both boundaries mark the edge of pervasive deep sea sill and flow overburden. It is suggested that this "rough/smooth boundary" was created by a fracture zone offset of the proto-Pacific/Farallon plate boundary.

5) The Ogasawara Fracture Zone acted as a focal point for Aptian-age and younger extrusive activity as indicated by the alignment and age of seamounts. There appears to be morphotectonic and geophysical evidence for both fracture zone and flexural effects within the broad region separating the PB and EMB. This feature has separated the two basins since at least 160 Ma.

6) Intrabasin morphotectonic structures other than seamounts, which could suggest a local (<100 km) source location for the extensive cover of deep sea sills and flows, are not evident on seismic or bathymetric records. However, the continuity of the sill/flow surface up the Caroline Ridge, the orientation of the "rough/smooth" Horizon B boundary, age and geochemical similarities between MORBs recovered in the Nauru Basin, EMB and the Ontong-Java Plateau suggest that the volcanism in these areas are closely related. We speculate that the deep sea sills/flows of varying thicknesses found in the EMB, southeast PB were locally emplaced through seamounts such as Ita Mai Tai with associated arch volcanism, and regionally emplaced along fissures/failed rifts which are manifested as subtle changes in depth and reflection character of volcanic basement.

Acknowledgement. This work was part of a joint U.S. - French effort to investigate the western Pacific basins. We wish to thank the ships crew and scientific party of the R/V Fred Moore (RIP) cruise FM35-12 and N/O Le Suroit. Perry Crampton and fellow airgun techs worked beyond the call of duty. Steffen Saustrup, Mark Wiederspahn, Patty Ganey at UTIG and Marc Schaming, Jacques Renault, Cecille Pourcellot and Roland Schlich at IPG, Strasbourg provided invaluable assistance in the processing of FM35-12 and MESOPAC II seismic data. John Mutter kindly donated the use of the L-DGO processing facilities during sonobuoy analysis. John Diebold contributed interactive software (JDSEIS), and along with Emilio Vera, provided helpful advice and discussion concerning sonobuoy data analysis/interpretation. Discussions with Nancy Grindlay, and Malcolm Pringle and reviews from Beth Ambos, Tom Brocher and Will Sager improved this paper. This project was funded by NSF grants OCE 86-13867 (R.Larson), OCE 86-13641 (T. Shipley) and from JOI/USSAC Ocean Drilling Fellowship (JSG-CY5-4) and a USSAC grant (20431) to the first author.

REFERENCES

Abrams, L.J., R.L. Larson, T. Shipley and Y. Lancelot, Cretaceous volcanic sequences and Jurassic(?) crust in the western Pacific, *Eos ,Trans. AGU, 69*, 1442, 1988.

Abrams, L.J., R. L. Larson, T. Shipley and Y. Lancelot, The seismic stratigraphy of the East·Mariana and Pigafetta Basins of the western Pacific, *Proc. ODP Sci. Res., 129*, 1992.

Asada, T., H. Shimamura, S. Asano, K. Kobayashi, and Y. Tomoda, Explosion seismological experiments on long-range profiles in the Northwestern Pacific and the Marianas Sea, in *The Ocean Basins and Margins*, Vol. 7A, edited by A. E. M. Nairn, Stehli, and S. Uyeda, 1985.

Batiza, R., Lithospheric age dependence of off-ridge volcano production in the North Pacific, *Geophys. Res. Lett., 8*, 853-856, 1981.

Brenner, C. and M. Angell, Bathymetric map of the East Mariana and Pigafetta Basins in the western Pacific, *Proc. ODP, Sci. Res., 129*, 1992.

Castillo, P. R., and R. W. Carlson, Possible origin of widespread Cretaceous volcanism in the Pacific: constraints from Sr, Nd, and Pb isotope geochemistry of Nauru Basin thoeliites, *Eos, Trans. AGU, 71*, 1667, 1990.

Castillo, P. R., and M. S. Pringle, Cretaceous volcanism in the western Pacific sampled at Sites 800 and 802, ODP Leg 129, *Eos, Trans. AGU, 72*, 300, 1991.

Castillo, P. R., P. A., Floyd, and C, France-Lanord, Isotope geochemistry of ODP Leg 129 basalts: Implications for the origin of a widespread volcanic event in the Pacific, *Proc. ODP Sci. Res., 129*, 1992.

Clague, D. A., R. T. Holcomb, J. M. Sinton, R. S. Detrick, and M. E. Torresan, Pliocene and Pleistocene alkalic flood basalts on the seafloor north of the Hawaiian islands, *Earth Planet. Sci. Lett., 98*, 175-191, 1990.

Courtillot, V. E., J. Besse, D. Vandamme, R. Montigny, J. J. Jeager, and H. Cappetta, Deccan flood basalts at the Cretaceous/Tertiary boundary?, *Earth Planet. Sci. Lett., 80*, 361-374, 1987.

Diebold, J. B., and P. L. Stoffa, The traveltime equation, tau-p mapping and inversion of common midpoint data, *Geophysics, 46*, 238-254, 1981.

Diebold, J. B., P. L. Stoffa, P. Buhl, and M. Truchan, Venezuela Basin Crustal Structure, *J. Geophys. Res., 86*, 7901-7923, 1981.

Edgar, N. T., and J. B. Saunders et al., *Init. Repts. DSDP, 15*: pp. 1137, 1973.

Ewing, J., M. Talwani, M. Ewing, and T. Edgar, Sediments of the Caribbean, in *International Conference on Tropical Oceanography Proc., 5*, pp. 88-102, Univ. of Miami, Miami, Fla., 1967.

Ewing, J., M. Ewing, T. Aitken, and W. J. Ludwig, North Pacific sediment layers measured by seismic profiling, in *The Crust and Upper Mantle of the Pacific Area*, edited by C. L. Drake, and P. J. Hart, pp. 147-173, AGU Monogr. Ser. v. 12, AGU, Washington, D. C., 1968.

Ewing, J. I., and G. M. Purdy, Upper crustal velocity structure in the ROSE area of the East Pacific Rise, *J. Geophys. Res., 87*, 8397-8402, 1982.

Floyd, P. A., P. R. Castillo, and M. S. Pringle, Tholeiitic and alkalic basalts of the oldest Pacific Ocean crust, *Terra Nova, 3*, 257-265, 1991.

Haggerty, J. A., and I. Primoli Silva et al., *Proc. ODP Init. Repts., 144:* College Station, TX (Ocean Drilling Program), in press, 1993.

Hamilton, E. L., Sunken islands of the Mid-Pacific Mountains, *Geol. Soc. Am. Mem., 64*, pp. 97, 1956.

Handschumacher, D. W., W. W. Sager, T. W. C. Hilde, and D. R. Bracey, Pre-Cretaceous tectonic evolution of the Pacific plate and extension of the geomagnetic polarity reversal time scale with implications for the origin of the Jurassic "Quiet Zone", *Tectonophysics, 155*, 365-380, 1988.

Harland, W. B., R. L. Armstrong, A. V. Cox, L. E. Craig, A. G. Smith, D. G. Smith, *A geologic time scale 1989*, 263 p., Cambridge Univ. Press, Cambridge, UK, 1990.

Heezen, B. C. and, I. D. MacGregor, et al., Mesozoic chalks beneath the Caroline abyssal plain: DSDP Site 199, *Init. Repts. DSDP, 20*, 65-85, 1973.

Hilde, T. W. C., Isezaki, N., and Wageman, J. M., Mesozoic seafloor spreading in the North Pacific, in *The Geophysics of the Pacific Ocean Basin and its Margins*, edited by G. H. Sutton, M. H. Manghnani, and R. Moberly, pp. 205-226, AGU Geophys. Monogr. Ser., vol. 19, 1976.

Houtz, R. E., J. Ewing, and P. Buhl, Seismic data from sonobuoy stations in the northern and equatorial Pacific, *J. Geophys. Res., 75*, 5093-5111, 1970.

Houtz, R., and J. Ewing, Upper crustal structure as a function of plate age, *J. Geophys. Res., 81*, 2490-2498, 1976.

Houtz, R. E., and W. J. Ludwig, Structure of Columbia Basin, Caribbean Sea, from profiler-sonobuoy measurements, *J. Geophys. Res., 82*, 4861-4868, 1977.

Houtz, R. E., and W. J. Ludwig, Distribution of reverberant subbottom layers in the southwest Pacific basin, *J. Geophys. Res., 84*, 3497-3505, 1979.

Hutchinson, D. R., and R. S. Detrick, Water gun vs air gun: a comparison, *Mar. Geophys. Res., 6*, 295-310, 1984.

Kroenke, L. W., and W. H. Berger et al., *Proc. ODP Init. Repts., 130*: College Station, TX (Ocean Drilling Program), pp. 1240, 1991.

Lancelot, Y., and R. L. Larson et al., *Proc. ODP Init. Repts., 129:* College Station, TX (Ocean Drilling Program), pp. 488, 1990.

Larson, R. L. and C. G. Chase, Late Mesozoic evolution of the western Pacific Ocean, *Geol. Soc. Am. Bull., 83*, 3627-3644, 1972.

Larson, R. L., Late Jurassic and Early Cretaceous evolution of the western central Pacific Ocean, *J. Geomag. Geoelectric., 28*, 219-236, 1976.

Larson, R. L. and, S. O. Schlanger, et al., *Init. Repts. DSDP, 61*: pp. 885, 1981.

Larson, R. L., Latest pulse of the Earth: Evidence for a mid-Cretaceous super plume, *Geology, 19*, 547-550, 1991a.

Larson, R. L., Geologic consequences of super plumes, *Geology, 19*, 963-966, 1991b.

Lincoln, J. M., M. S. Pringle, and I. Primoli Silva, Early and Late Cretaceous volcanism and reef-building in the Marshall Islands: New fossil evidence and Ar^{40}/Ar^{39} ages, this volume.

Lipman, P. W., D. A. Clague, and R. T. Holcomb, South arch volcanic field - newly identified young lava flows on the sea floor south of the Hawaiian Ridge, *Geology, 17*, 611-614, 1989.

Lowrie, A., C. N. Smoot, and R. Batiza, Are oceanic fracture zones strong or weak? New evidence for volcanic activity and weakness, *Geology, 14*, 242-245, 1986.

Macdonald, K. C., Mid-ocean ridges: Fine scale tectonic, volcanic and hydrothermal processes within the plate boundary zone, *Ann. Rev. Earth Planet. Sci., 10*, 155-190, 1982.

Mahoney, J. J., and J. A. Tarduno, Cretaceous volcanism and the formation of the Ontong-Java plateau: New insights from ODP Leg 130, *Eos, Trans. AGU, 71*, 1668, 1990.

Mammerickx, J., and G. F. Sharman, Tectonic evolution of the North Pacific during the Cretaceous quiet period, *J. Geophys. Res., 93*, 3009-3040, 1988.

Menard, H. W., *Marine Geology of the Pacific*, pp. 271, McGraw Hill Book Co., New York, NY, 1964.

Moberly, R., and S. O. Schlanger et al., *Init. Repts. DSDP, 89*, pp. 678, 1986.

Nakanishi, M., K. Tamaki, and K. Kobayashi, Mesozoic magnetic anomaly lineations and seafloor spreading history of the northwestern Pacific, *J. Geophys. Res., 94*, 15,437-15,462, 1989.

Nakanishi, M., K. Tamaki, and K. Kobayashi, Magnetic anomaly lineations from Late Jurassic to Early Cretaceous in the west-central Pacific Ocean, *Geophys. J. Int., 109*, 701-719, 1992.

Ozima, M., I. Kaneoka, K. Saito, M. Honda, M. Yanagisawa, and Y. Takigami, Summary of geochronological studies of submarine rocks from the western Pacific Ocean, in *Geodynamics of the western Pacific-indonesian region, v.11*, edited by T .W .C. Hilde, and S. Uyeda, 137-142, 1983.

Pringle, M. S., Radiometric ages of basaltic basement recovered by ODP Leg 129, *Proc. ODP Sci. Res., 129*, 1992a.

Pringle, M. S., Geochronology and petrology of the Musicians Seamounts and the search for hot spot volcanism in the Cretaceous Pacific, (Ph.D. dissertation), University of Hawaii, Honolulu, 1992b.

Purdy, G. M., The seismic structure of 140 my old crust in the Central Atlantic Ocean, *Geophys. J. R. Astron. Soc., 72*, 115-138, 1983.

Sager, W. W., D. W. Handschumacher, T. W. C. Hilde, and D. R. Bracey, Tectonic evolution of the northern Pacific plate and Pacific - Farallon - Izanagi triple junction in the Late Jurassic and Early Cretaceous (M21-M10), *Tectonophysics, 155*, 345-364, 1988.

Schubert, G., and D. Sandwell, Crustal volumes of the continents and of oceanic plateaus and continental submarine plateaus, *Earth Planet. Sci. Lett., 92*, 234-246, 1989.

Shipley, T. H., J. M. Whitman, F. K. Duennebier, and L. D. Peterson, Seismic stratigraphy of the East Mariana Basin, western Pacific, *Earth Planet. Sci. Lett., 64*, 257-275, 1983.

Shipley, T. H., L. J. Abrams, R. L. Larson, and Y. Lancelot, Extent of Cretaceous volcanic sequences in the Jurassic Nauru Basin, western Pacific, this volume.

Smith, W. H. F., H. Staudigel, A. B. Watts, and M. S. Pringle, The Magellan Seamounts: Early Cretaceous record of the South Pacific isotopic and thermal anomaly, *J. Geophys. Res., 94*, 10,501-10,523, 1989.

Spudich, P., and J. A. Orcutt, A new look at the seismic velocity structure of the oceanic crust, *Rev. Geophys. Space Phys., 18*, 627-645, 1980.

Steiner, M., J. Ogg, and J. Sandoval, Jurassic magnetostratigraphy, 3. Bathonian-Bajocian of Carcabuey, Sierra Harana and Campillo de Arenas (Subbetic Cordillera southern Spain), *Earth Planet. Sci. Lett., 82*, 357-372, 1987.

Talwani, M., C. C. Windisch, P. L. Stoffa, P. Buhl, and R. E. Houtz, Multi-channel seismic study in the Venezuelan Basin and the Curacao ridge, in *Island Arcs, Deep Sea Trenches and Back-Arc Basins*, edited by M. Talwani, and W. C. Pitman, pp. 83-98, AGU Monogr. M. Ewing Ser. v. 1, 1977.

Tamaki, K. and R. L. Larson, The Mesozoic tectonic history of the Magellan microplate in the Western Central Pacific, *J. Geophys. Res., 93*, 2857-2874, 1988.

Tamaki, K., M. Nakanishi, K. Sayanagi and K. Kobayashi, Jurassic magnetic anomaly lineations of the Western Pacific and the origin of the Pacific plate, *Eos, Trans. AGU, 68*, 1493, 1987.

Tarduno, J. A., W. V. Sliter, L. Kroenke, M. Leckie, H. Mayer, J. J. Mahoney, R. Musgrave, M. Storey, and E. L. Winterer, Rapid formation of the Ontong-Java Plateau by Aptian mantle plume volcanism, *Science, 254*, 399-403, 1991.

Thiede, J., and T. L. Vallier et al., *Init. Repts. DSDP, 62*, pp. 1120, 1981.

Vogt, P. R., Volcano spacing, fractures and thickness of the lithosphere, *Earth Planet. Sci. Lett., 21*, 235-252, 1974.

Weissel, J. K. and R. N. Anderson, Is there a Caroline plate?, *Earth Planet. Sci. Lett., 41*, 143-158, 1978.

Wipperman, L. K., R. L. Larson, and D. M. Hussong, The geological and geophysical setting near site 462, *Init. Repts. DSDP, 61*, 763-770, 1981.

Winterer, E. L., and J. Ewing et al., *Init. Repts. DSDP, 17*:, pp. 930, 1973.

Winterer, E. L., Anomalies in the tectonic evolution of the Pacific, in *The Geophysics of the Pacific Ocean Basin and its Margin*, edited by G. H. Sutton, M. H. Manghnani, and R. Moberly, pp. 269-278, AGU Monogr. Ser. v. 19, AGU, Washington, D.C., 1976.

Winterer, E. L., Duncan, R. A., McNutt, M. K., Natland, J. H., Premoli Silva, Isabella, Sager, W. W., Sliter, W. V., Van Waasbergen, R., and Wolfe, C. J., Cretaceous guyots in the northwest Pacific: An overview of their geology and geophysics, this volume.

White, R. S., Oceanic upper crustal structure from variable angle seismic reflection - refraction profiles, *Geophys. J. R. astr. Soc., 57*, 683-726, 1979.

White, R. S., Atlantic oceanic crust: seismic structure of a slow-spreading ridge, in *Ophiolites and Oceanic Lithosphere*, edited by I. G. Gass, S. J. Lippard and A. W. Shelton, pp. 101-111 Geol. Soc. London, 1984.

L. J. Abrams, now at Department of Geology, University of Puerto Rico, P.O. Box 5000, Mayaguez, PR 00709.

R. L. Larson, Graduate School of Oceanography, University of Rhode Island, Narragansett, RI 02882.

T. H. Shipley, Institute for Geophysics, University of Texas, Austin, TX 78759.

Y. Lancelot, Laboratoire de Geologie du Quaternaire, CNRS-Luminy, Case 907, 13288 Marseille, Cedex 9, France.